Royal Netherlands
Meteorological Institute
Ministry of Infrastructure and the Environment

Validation and evaluation of SEVIRI volcanic ash heights

A.T.J. de Laat and R.J. van der A

De Bilt, 2012 | Technical report; TR-337

Validation and evaluation of SEVIRI volcanic ash heights.

Version 1.0

Date 10 December 2012
Status Final

Colofon

Title	Validation and evaluation of SEVIRI volcanic ash heights.
Projectleader	Dr. R.J. van der A — T (+31) 030 2206 412 Royal Netherlands Meteorological Institute (KNMI)
Contact	Dr. A.T.J. de Laat T (+31) 030 2006 892 F (+31) 030 2210 407 laatdej@knmi.nl Royal Netherlands Meteorological Institute (KNMI) Wilhelminalaan 10 3732 GK de Bilt The Netherlands
Author	A.T.J. de Laat — T (+31) 030 2206 892

Contents

Colofon — 5
Contents — 7

1 Introduction — 9

2 Methods — 11
2.1 SEVIRI instrument — 11
2.2 SEVIRI volcanic ash detection — 11
2.2 SEVIRI volcanic ash height — 12

3 Evaluation and validation — 16
3.1 CALIPSO/CALIOP — 16
3.2 Comparison SEVIRI and CALOP — 17
3.3 Summary comparison SEVIRI and CALIOP ash heights — 19
3.4 GOME2 FRESCO cloud top heights — 19

4 Summary and conclusions — 22

5 References — 23

6 Auxiliary information — 24
Captions — 24
Table S1 — 25
Figures S1 — 26-30
Figures S2 — 31-42
Figures S2 — 43-59

1 Introduction

The April-May 2010 eruptions of the Icelandic volcano Eyjafjallajokull provided a clear example of the disruptive effects volcanic eruptions can have on modern society. Due to the closure of European air space because of volcanic ash plumes, millions of travelers were stranded and air travel in, from and to Europe was disrupted for days to weeks. In the aftermath of the episode it became clear that on the one hand European regulations may have been too strict, while on the other hand there was a need for easy access to all available satellite information on volcanic ash.

For the European Volcanic Observatory Space Services project (EVOSS), this eruption could not have been more fortuitous with its kick-off in March 2010. The principal goal of EVOSS is to develop and demonstrate a portfolio of services based on earth observation products for monitoring volcanic activity and related hazards on a global scale.

One of the important products of this project is to make volcanic ash information derived from geostationary satellites available. Geostationary satellites have the advantage that they provide continuous information on the location of volcanic ash plumes, and thus are important for near-real time monitoring and potentially crucial for aviation industry. Research into the possibilities to retrieve information on volcanic ash from geostationary satellites – in particular quantitative information - had been going for quite some time, and at the moment of the Eyjafjallajokull eruption it was clear the current algorithm were sufficiently advanced for practical use.

Due to the political and societal recognition of satellite measurements as an important information source, EVOSS and the EUropean METeorological SATellite (EUMETSAT) organization quickly joined forces in order to make geostationary volcanic ash information available via the EVOSS service available. EUMETSAT had already initiated a pilot study into the capacity of a near-real-time service on volcanic ash, which led to the release of a report in April 2011 [Prata, 2011]. The main findings of the report were that quantitative information on volcanic ash could be retrieved from measurements of the Spinning Enhanced Visible and InfraRed Imager (SEVIRI), most importantly volcanic ash mass loading and ash height.

In parallel to the assessment of the EUMETSAT product, KNMI developed its own ash height product. Reason for doing so was on the one hand that at the time of the assessment it was unclear whether or not EUMETSAT was allowed to make its information available, and on the other hand there was an alternative to the methodology for calculation ash heights as done by EUMETSAT (see method section).

However, although EUMETSAT has implemented the Prata [2011] algorithm, which it dubbed “VOLE” and provides near-real time data, the quality of both the mass loading and ash height had yet to be determined. For the first task another pilot study was launched, and results were recently published [Prata and Prata, 2012]. The validation of ash heights was incorporated within the EVOSS work packages, and results from the validation study will be presented in this report.

2 Methods

2.1 SEVIRI instrument

We will only provide a brief description of the SEVIRI instrument. More detailed information can be found in Schmetz et al. [2002] and the EUMETSAT website (http://www.eumetsat.int/Home/Main/Satellites/MeteosatSecondGeneration/Instruments/index.htm). SEVIRI has 12 narrow-band channels (width ~ 1 μm) covering the visible (VIS) and infrared (IR) regions of the electromagnetic spectrum. For volcanic ash retrievals only the 5 channels between 6.2 and 12.0 μm are important. The SEVIRI instrument is in a geosynchronous orbit approximately over 0° longitude and 0° latitude. The total field of view is approximately 70° providing coverage of the earth from about 70°S to 70°N and 70°W to 70°E. There are 3712×3712 pixels covering the full disk.

2.2 SEVIRI volcanic ash detection

The prime reason that the SEVIRI measurements contain information about volcanic ash is that the extinction coefficients for silicates exhibit a wavelength dependence. Therefore, brightness temperatures of the 10.8μm and 12.0μm channels differ slightly in the presence of volcanic ash. Furthermore, it turns out that this wavelength dependence differs between silicates on the one hand and water vapor and ice on the other hand. As a result, not only can volcanic ash be detected, volcanic ash clouds can also be distinguished from water vapor clouds. For a more detailed description see chapters 3 of Prata [2011].

Further investigation of this effect has shown that, by using complex radiative transfer calculations, quantitative information on the mass loading can be derived. By combining information on cloud top heights, surface and brightness temperatures and their differences an estimate for the mass loading can be derived. For a fast algorithm pre-processed lookup-tables are prepared so that for a given combination of parameters a mass load can be found.

An example of such a lookup table is given in figure 1. This figure shows the mass loading as a function of brightness temperature and brightness temperature differences a certain atmospheric conditions. There are two effects typical for the detection of volcanic ash using this methodology and these channels. One is the U-shape that is the non-linear dependence of the mass loading as a function of brightness temperature. The other one is the non-linearity of the mass loading as a function of brightness temperature difference, *i.e.* that the largest mass loadings do not coincide with the largest brightness temperature differences. The latter provides important limitations, as will be discussed later on. Nevertheless, Prata and Prata [2012] showed that, given that atmospheric volcanic ash loadings can vary orders of magnitude, validation results show a good agreement between the mass loading derived from satellites and other instruments and measurements. As a result, the satellite estimates of mass loads are sufficiently accurate for practical use. For an extensive description of the physics behind this method and the method itself, we refer to Prata [2011], Prata and Prata [2012] and references therein.

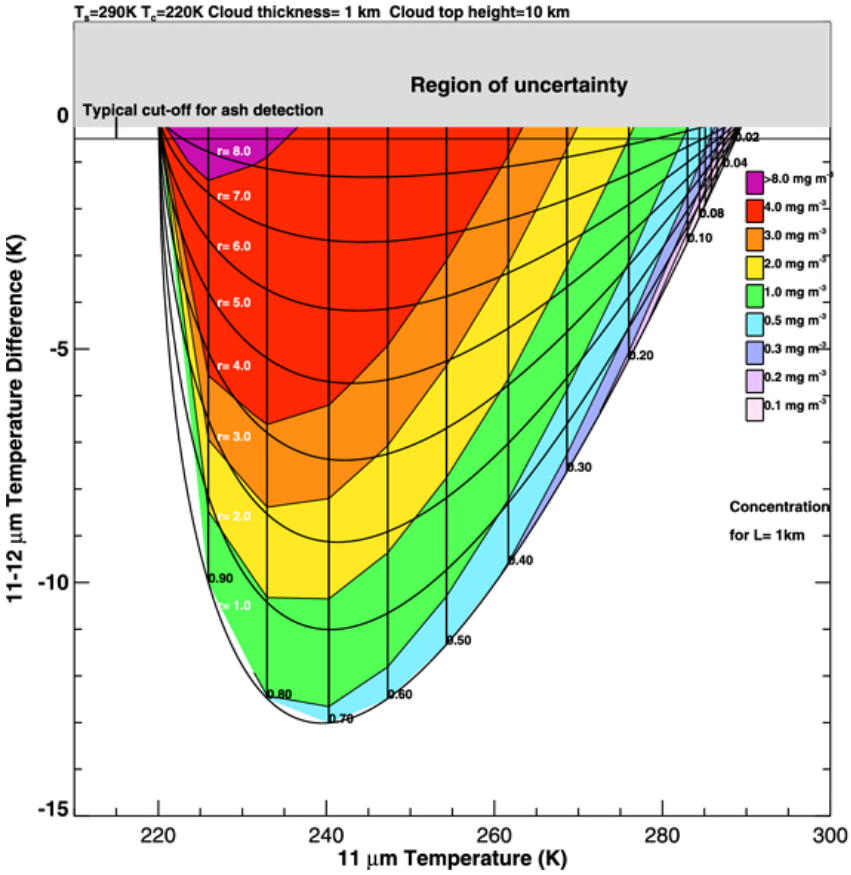

Figure 1. *After figure 2 of Prata and Prata [2012]. The colored regions show ash concentrations (mg m^{-3}). The near-vertical lines are isolines of optical depth, the parabolas are isolines of effective radius. The intersection of a line of 11 μm brightness temperature with a line of ΔT provides an estimate of the ash concentration, assuming a cloud thickness of 1 km. In practice a different chart can be selected from a set that have been pre-computed to cover a range of realistic cloud top height temperatures and surface temperatures. For this case the cloud top temperature is 220 K (10 km high cloud) and the surface temperature is 290 K.*

2.3 SEVIRI volcanic ash detection

An important parameter for the quantitative volcanic ash retrievals from SEVIRI is the ash cloud top temperature (Tc). In order to maintain speed and simplicity of the retrieval scheme, the ash cloud top temperature is estimated from SEVIRI data. The procedure for this works as follows [Tim Hultberg, EUMETSAT, personal communication, 25 May 2012]:

For the estimation of the ash cloud top temperature, the 3712×3712 image is divided into 128×128 blocks of size 29×29 pixels each.

1. Determine the minimum value of the 12.0 μm channel brightness temperature channel for potentially ash contaminated pixels within each block.
2. Within each block set Tc to the minimum value of T12.0 in a region of 15×15 blocks centered around the current block

The ash height then subsequently is determined by calculating the height given a predicted surface skin temperature and assuming a 7 K/km lapse rate.

The motivation for this procedure is given by the need of the retrieval of mass loading for an estimate of the ash height. The calculation of mass-loading itself turns out not to be overly sensitive to the actual ash height [Prata, 2011]. However, for the determination of ash height this procedure has some disadvantages, most notably the need for a large number of pixels and selection within a large area.

As an alternative, the KNMI algorithm first determines if a pixel likely contains volcanic ash. This is done by calculating the brightness temperature difference between the 12.0 μm and 10.8 μm channels and the 10.8 μm and 8.7 μm channels ($\Delta T_{12.0\text{-}10.8}$ and $\Delta T_{10.8\text{-}8.7}$). Positive volcanic ash identification occurs when $\Delta T_{12.0\text{-}10.8}$ > 1K and $\Delta T_{10.8\text{-}8.7}$ < 5K and the actual brightness temperature of the 10.8 μm channel is less than 300K. This is a slightly more strict filter used by EUMETSAT as we want to avoid too many false positives occurring predominantly over desert regions and high zenith angles. Using (re)analysis data from the European Center for Medium range Weather Forecast (ECMWF) the corresponding altitude is determined from the 10.8 μm brightness temperature and the local ECMWF temperature profile.

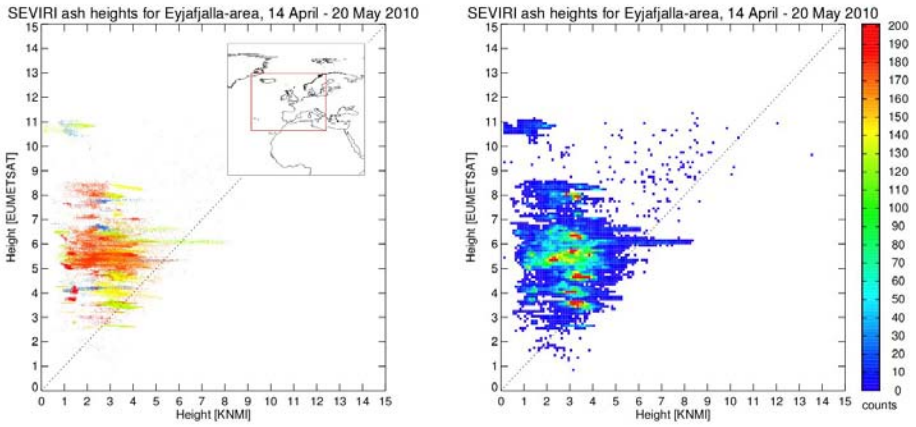

Figure 2. *Comparison of EUMETSAT and KNMI as heights for the period 14 April – 20 May 2010 for the region 30°W-20°E and between 30°N-70°N (see insert in left panel). The left plot shows all data, where colors indicate different days, the right plot the corresponding probability distribution. Heights are in km.*

As a first test, we show the collocated KNMI and ECMWF ash heights. These comparisons are based on pre-selected times for which the ash plumes coincided with a CALIPSO overpass. This list of CALIPSO overpasses was presented in Prata [2011] and can be found in the auxiliary information (table S2).

Figure 2 shows the comparison between ash heights from both the EUMETSAT and KNMI. Clearly there is little correspondence between both: the EUMETSAT data shows a much larger range of values (up to 11 km), whereas the KNMI product suggests few ash heights above 6 km altitude. Another striking difference is the range of values for individual days. It appears that the EUMETSAT product shows a close to constant altitude range for individual days (and thus ash plumes) compared

to the KNMI product. These results already show that the two methods provide significantly different results. The most likely explanation is that the EUMETSAT method is unsuitable for a physically realistic detection of ash heights, as it effectively uses the lowest brightness temperature as ash-height estimate for ash-pixels within a very large area. The EUMETSAT ash heights will vary around the height of the lowest brightness temperature due to variations in surface (skin) temperature.

To further investigate the quality of the EUMETSAT ash heights, we also show a cross section of a CALIOP orbit (12 May 2010; see next section and auxiliary information for more on the comparison with CALIOP) with corresponding SEVIRI heights and mass loading in Figure 3, which consists of three panels for both the EUMETSAT and KNMI ash heights. Indicated in the top panel is the CALIOP vertical feature mask, with light blue indicating clouds, and orange indicating aerosols, and the corresponding mean ash for all SEVIRI volcanic ash heights within a 100 km radius around the CALIOP measurement as well as the root-mean-square of these collocated ash heights in white. The middle panel is similar to the top panel but without the CALIOP vertical feature mask. The lowest panel shows the corresponding number of SEVIRI volcanic ash pixels within the 100 km radius distance around the CALIOP measurement, and the corresponding average mass loading.

The EUMETSAT heights show little variations, despite the presence of a large number ash pixels within the 100 km radius distance. Only for a small region there is more variability. The KNMI heights, on the other hand, show much more variability (large root-mean-square value) for most collocations, reflecting much more ash height variability within the ash plume.
These findings are consistent with the notion that the EUMETSAT ash heights likely show too little variability and thus are not really representative for the true ash heights. It also explains the limited variability in the EUMETSAT product on a day-to-day basis (Figure 2).

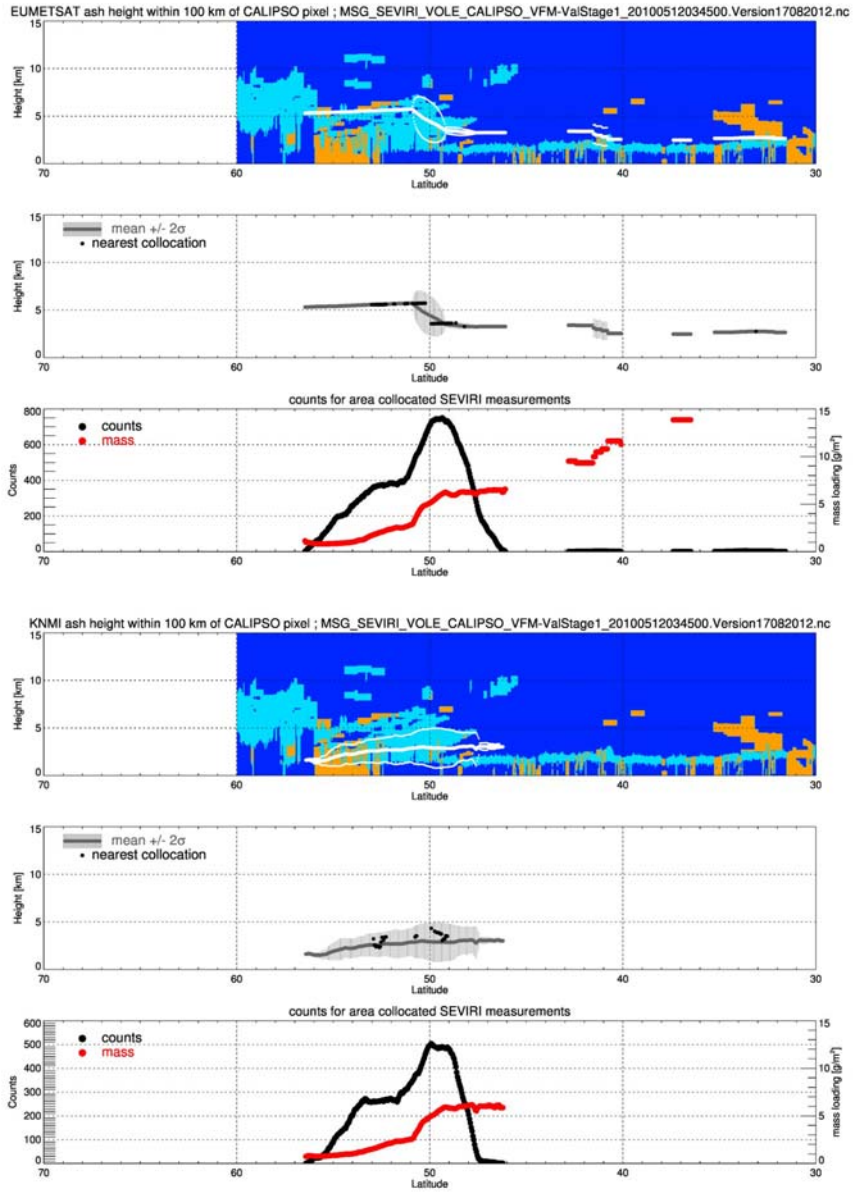

Figure 3. *SEVIRI collocated ash heights (EUMETSAT, upper three panels; KNMI, lower three panels) and mass loading (in both plots EUMETSAT) for a CALIOP overpass of the ash plume on 12 May 2010. The light blue colors in the first and fourth panel indicate a cloud, the orange colors indicate aerosols. Other CALIOP features types are not included (dark blue).*

3 Evaluation and validation

3.1 CALIPSO/CALIOP

For the evaluation of ash heights we use measurements from the CALIOP lidar for comparison. The CALIOP lidar provides vertical information on clouds and ash. For a detailed description of CALIOP we refer to the CALIPSP website of the French Centre National d'Etudes Spatiales (CNES; http://smsc.cnes.fr/CALIPSO/).

For the automated detection of ash and clouds, we use the lidar Vertical Feature Mask scientific dataset (VFM). The VFM data product contains scene classification data, including identifiers for clouds, cloud types, aerosol and aerosol types.

Figure 4 shows the SEVIRI (VOLE) mass loading over the Northern Atlantic on 12 May 2010, and the corresponding CALIOP track. Clearly the CALIOP track crosses right through a long volcanic ash plume.

Figure 5 presents an example of a CALIOP "curtain plot", showing reflectance signatures as a function of height. As can be seen from the CALIOP measurements, the ash plume consists of multiple layers. The corresponding SEVIRI ash heights coincide with parts of the plume, but it is obvious that one cannot define one particular ash height.

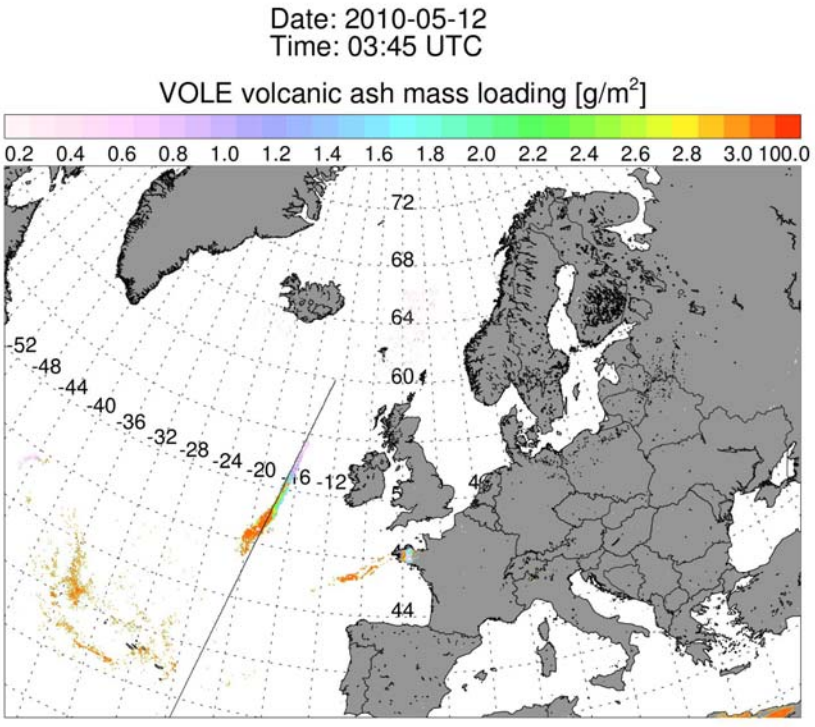

Figure 4. *SEVIRI volcanic ash mass loading from the EUMETSAT VOLE product for 12 May 2010, 03:45 UTC. The dark line indicates a CALIOP orbit track.*

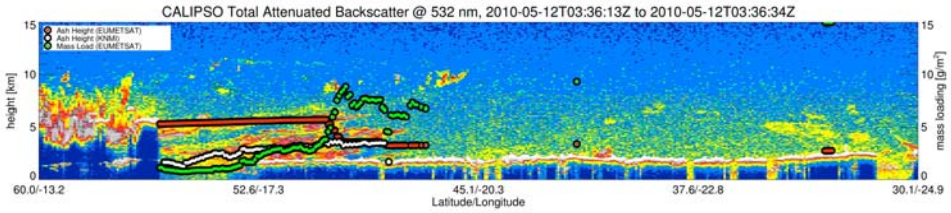

Figure 5. *CALIOP total attenuated backscatter for the orbit shown in Figure 4. Indicated are also the collocated SEVIRI ash height (EUMETSAT, red; KNMI, white) and the SEVIRI mass loading (green).*

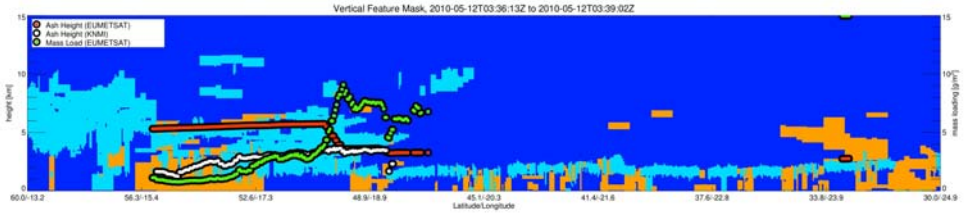

Figure 6. *CALIOP vertical feature mask for the same orbit as shown in Figure 4. The light blue color indicates a cloud, the orange color indicates aerosols. Other CALIOP features types are not shown (dark blue).*

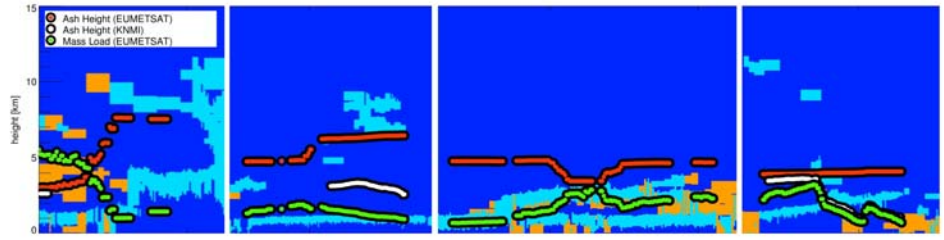

Figure 7. *A selection of CALIOP vertical feature mask scenes and collocated SEVIRI ash heights and mass loadings.*

If we further investigate the CALIOP vertical feature mask for the same orbit, we see that CALIOP has difficulties distinguishing whether or not the volcanic ash cloud consists mainly of ash or of water vapour. The identifiers for aerosol-subtypes – not shown here – also do not provide much additional information.

Figures 5 and Figure 6 further reveal another feature of the SEVIRI ash heights: there appears to be a correlation between VOLE ash heights and mass loadings. The VOLE as height shows a decrease in height at the same time the mass loads increase. Figure 7 shows a sample of other scenes where interdependencies were seen.

3.2 Comparison SEVIRI and CALIOP

Figure 8 presents a summary of the SEVIRI volcanic ash and CALIOP cloud and aerosol heights for CALIOP measurements coinciding with SEVIRI (collocation distance < 5 km). We simply used the CALIOP vertical feature mask, and for both "clouds" and "aerosols" calculated the average height. Note that CALIOP has a

horizontal resolution of 300 meter and a vertical resolution of 30 meter (from the

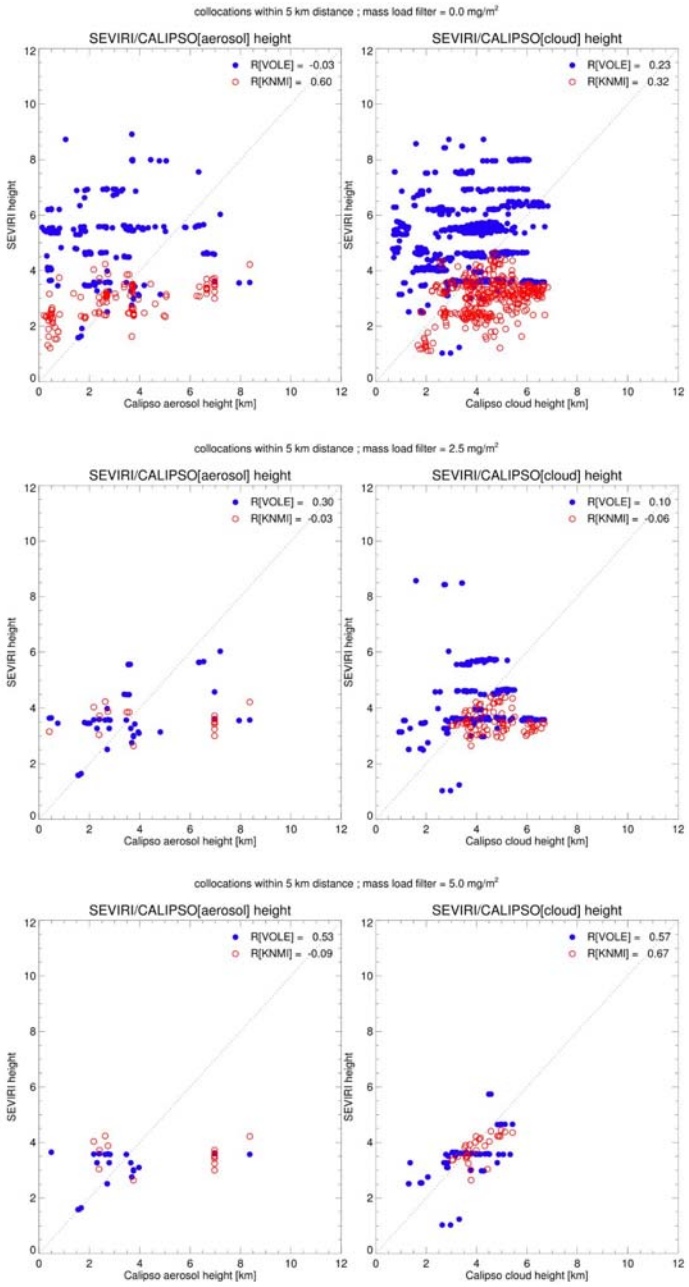

Figure 8. *Comparison between SEVIRI (VOLE, KNMI) and CALIOP heights (aerosols, clouds). The upper panel shows all collocated data (mass load > 0.0 mg/m^2). The middle and lower panels show collocated data for mass loads larger than 2.5 and 5.0 mg/m^2, respectively).*

surface up to 8.2 km altitude) and 60 meter (between 8.2 and 15 km altitude). Figure 8 shows three panels based on the SEVIRI mass load (> 0.0, > 2.5 and > 5 mg/m^2). As can be seen, correlations between SEVIRI and CALIOP are in general not good for either CALIOP aerosols or clouds. Only for the most dense ash clouds (mass load > 5 mg/m^2) there appears to be some correspondence between SEVIRI

and either CALIOP clouds or aerosols. This provides a small hint that for optically thick ash clouds the height algorithms may provide some information. Note that, similar to previous comparisons, the VOLE heights are organized in "bands", i.e. little variation from day to day. This appears to be confirmed by careful inspection of all CALIOP-SEVIRI comparisons (see auxiliary figures S3). However, the number of CALIOP collocations with SEVIRI pixels with larger ash mass loadings is rather limited due to the limited spatial coverage of CALIOP.

3.3 Summary comparison SEVIRI and CALIOP ash heights

The comparison between SEVIRI and CALIOP ash heights does not provide encouraging results. In general, no correlations are found, except for high mass loads. Furthermore, we found that the VOLE ash height is not independent from VOLE mass loading.

However, the use of CALIOP data has clear limitations, as the CALIOP VFM appears not suitable for the detection of volcanic ash. In addition, it appears that the volcanic plume itself is a mixture of ash and water vapour. The latter should not come as a surprise, as the Eyjafjallajokull volcano is covered with glaciers, snow and ice. Nevertheless, the combined ash-water composition of the volcanic plume hampers validation of SEVIRI ash heights with CALIOP, and other means of evaluating SEVIRI ash heights must be explored.

For a complete overview of all SEVIRI-CALIOP comparisons, as well as a list of CALIOP orbits used for the comparison, we refer to the auxiliary information.

3.4 GOME2 FRESCO cloud top heights

As an alternative method for the evaluation of volcanic ash heights a comparison with GOME2 FRESCO (version 6) cloud top heights was made. The GOME2 FRESCO algorithm provides cloud top heights derived from the O_2-A absorption band around 760 nm. Recently, it was shown that FRESCO algorithm is also capable of determining the heights of optically thick ash clouds originating from fires or volcanic eruptions [de Laat et al., 2012; Wang et al. 2012, and references therein for a detailed description of the FRESCO algorithm]. Since the volcanic ash clouds also can be seen in Absorbing Aerosol Index (AAI) measurements from GOME2, combining AAI measurements with FRESCO measurements provides an alternative database for comparison with SEVIRI ash heights.

There are some caveats with this method. First of all, the spatial resolution of GOME2 (80×40 km) is considerable larger than the typical SEVIRI pixel (5-10 km). This is something to consider when comparing both. Another issue is that for optically thin clouds the method does not work. This could be done by filtering on AAI values, but it should be kept in mind that the AAI also depends on altitude (the higher aerosol layer, the higher its AAI value will be for similar aerosol optical depths).

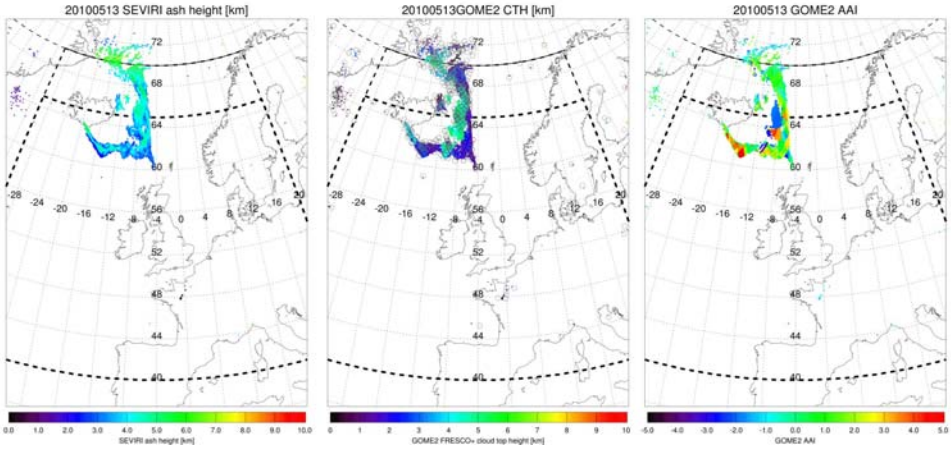

Figure 9. *SEVIRI (KNMI) volcanic ash height (left panel) collocated with GOME2 FRESCOv6 cloud top heights (middle panel) and GOME2 absorbing aerosol index (right panel) for 13 May 2010. Indicated in the middle panel are also the central longitude and latitude of the GOME2 pixels. Every SEVIRI measurement is attributed to the nearest GOME2 measurements. Dotted lines are for comparison purposes.*

Figure 9 shows an example of such a comparison. GOME2 cloud top height and AAI measurements are collocated on a pixel-to-pixel basis. Combining all SEVIRI and GOME2 measurements for the entire Eyjafjallajokull eruption period lead is shown in Figure 10. When filtering for thicker ash clouds, there is a reasonable correlation between GOME2 FRESCOv6 cloud top height and SEVIRI ash height. Note that SEVIRI ash heights appear to be systematically higher than GOME2 cloud top heights. This could be explained by the fact that SEVIRI determines cloud tops based on InfraRed measurements, and thus cloud top altitudes close to the physical edge of the clouds, whereas GOME2 determines cloud tops from UV/VIS measurements and also obtains information from within the cloud (effectively lower the cloud top estimate). It is thus not unexpected that SEVIRI ash heights are somewhat higher in altitude than GOME2 FRESCOv6 cloud heights. Combined with the considerable differences in pixels size between GOME2 and SEVIRI, we conclude that the KNMI SEVIRI ash heights are doing a reasonable job. However, given the large spread in the data in the left hand plot, care has to be taken with the use of GOME2 FRESCOv6 cloud top heights in case of volcanic eruptions. For a complete overview of all available days and comparisons we refer to the auxiliary information.

SEVIRI determines cloud tops based on InfraRed measurements, and thus cloud top altitudes close to the physical edge of the clouds, whereas GOME2 determines cloud tops from UV/VIS measurements and also obtains information from within the cloud (effectively lower the cloud top estimate). It is thus not unexpected that SEVIRI ash heights are somewhat higher in altitude than GOME2 FRESCOv6 cloud heights. Combined with the considerable differences in pixels size between GOME2 and SEVIRI, we conclude that the KNMI SEVIRI ash heights are doing a reasonable job. However, given the large spread in the data in the left hand plot, care has to be taken with the use of GOME2 FRESCOv6 cloud top heights in case of volcanic eruptions. For a complete overview of all available days and comparisons we refer to the auxiliary information.

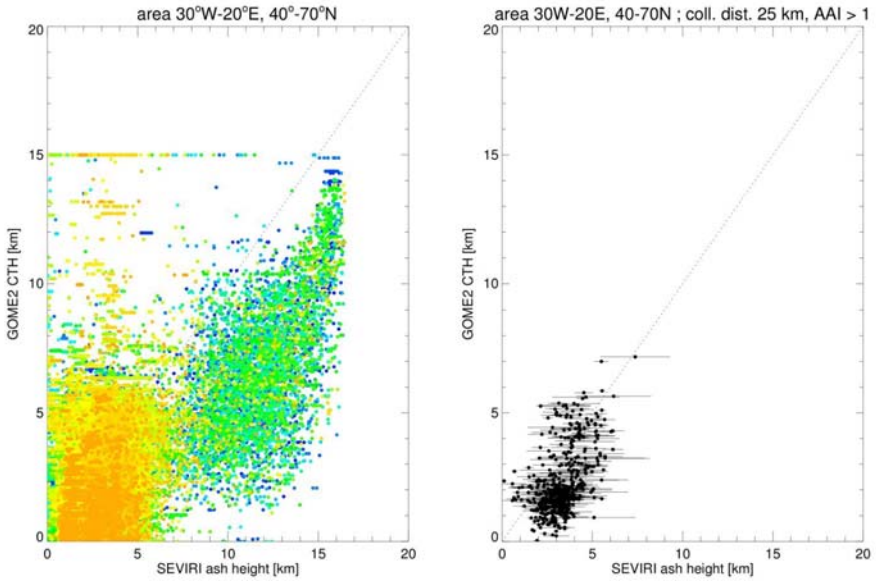

Figure 10. *Comparison between SEVIRI (KNMI) and collocated GOME2 FRESCOv6 cloud top heights for the period 14 April -20 May 2010. The left panel shows all collocated data for the Eyjafjalla-area 30°W-20°E and 40°N-70°N. Color coding indicates the date (April-May goes from blue to green to yellow to orange). The right panel is the same as the left panel but only for AAI values > 1, and for collocation distances between the centre of the SEVIRI and GOME2 pixels < 25 km. The error bars for the SEVIRI ash heights in the right plot indicate the 2σ value of the SEVIRI measurements for each GOME2 pixel.*

4 Summary and conclusions

In this report we have presented results from the validation/evaluation of SEVIRI volcanic ash heights from the "official" EUMETSAT algorithm (VOLE), and the KNMI ash heights based on both SEVIRI and ECMWF data. The CALIOP Vertical Feature Mask and GOME2 FRESCOv6 cloud top heights were used for the comparison.

The direct comparison of both SEVIRI ash height products showed already large differences and discrepancies. For the VOLE heights, these discrepancies are likely related to the algorithm, which really is not tailored for the accurate determination of volcanic ash heights. As a result, use of VOLE ash heights should be avoided.

The comparison between CALIOP and SEVIRI indicates that CALIOP has difficulties discriminating volcanic ash from other features. To some extent this could be related to the mixed ash-droplet volcanic plumes from this particular eruption. Only for the optically very thick volcanic ash clouds we found indications that there was a correspondence between CALIOP and SEVIRI. Nevertheless, CALIOP data was judged unsuitable for an automated objective validation of SEVIRI volcanic ash heights.

Comparison between SEVIRI-KNMI volcanic ash heights and GOME2 FRESCOv6 cloud top heights revealed a reasonable agreement for optically thick clouds. Given the differences in pixel size between the two instruments and the different wavelengths where both instrument determine heights (InfraRed for SEVIRI, UV/VIS for GOME2), we conclude that SEVIRI can provide information on volcanic ash heights. However, given that this is the first time these SEVIRI ash height products have been evaluated, we urge users to always consult additional data sources when using SEVIRI ash heights.

Finally, for SEVIRI current efforts with regard to measuring volcanic ash by European space research focus on improving on the current algorithm and combining or integrating the VOLE and KNMI methodology in a better algorithm. For GOME2 and TROPOMI, efforts are underway to investigate if the O_2-A band combined with other UV/VIS wavelengths contain vertical information on ash heights and ash layer thickness. The latter would potentially enable determination of ash concentrations rather than ash mass loadings, where the former is preferred by aviation industry. The possible presence of an O_2-A band on the geostationary sentinel-4 instrument could then further enhance observing capacity of volcanic ash over the larger European area, as it would provide hourly updates.

5 References

de Laat et al. (2012), A solar escalator: Observational evidence of the self-lifting of smoke and aerosols by absorption of solar radiation in the February 2009 Australian Black Saturday plume, J. Geophys. Res., 117, D04204, doi:10.1029/2011JD017016.

Prata (2011), Volcanic information derived from satellite data, EUMETSAT volcanic ash and SO_2 pilot project report, April 18 2011, available on request via EUMETSAT.

Prata, A. J. and A. T. Prata (2012), Eyjafjallajökull volcanic ash concentrations determined using Spin Enhanced Visible and Infrared Imager measurements, J. Geophys. Res., 117, D00U23, doi:10.1029/2011JD016800.

Schmetz, J., et al. (2002) An Introduction to Meteosat Second Generation (MSG). Bull. Amer. Meteor. Soc., 83, 977–992.m doi: http://dx.doi.org/10.1175/1520-0477(2002)083<0977:AITMSG>2.3.CO;2

Wang et al. (2012), Interpretation of FRESCO cloud retrievals in case of absorbing aerosol events, Atmos. Chem. Phys., 12, 9057-9077, doi:10.5194/acp-12-9057-2012.

6 Auxiliary information

Captions

Table S1

CALIPSO-SEVIRI coincidences during April/May 2010.

Figure series S1-##

Spatial distribution of SEVIRI-EUMETSAT (VOLE) mass loading (g/m^2). Indicated are also CALIOP orbits (black line), based on the CALIOP orbits listed in table S2, and corresponding SEVIRI measurements. Indicated below each panel is the CALIOP orbit signature, which are also shown in Figure series S3.

Figure series S2-##

CALIOP total attenuated backscatter (first of every two panels), vertical feature mask (second of every two panels) and corresponding SEVIRI ash height (in km; EUMETSAT, red, KNMI, white) and SEVIRI mass load (in g/m^2; EUMETSAT, green) for the same measurements as shown in Figure series S2. In the vertical feature mask panels, the light blue color indicates a cloud, the orange color indicates aerosols. Other features types are not shown (dark blue).

Figure series S3-##

Spatial distribution of SEVIRI-KNMI ash height (upper left plot), corresponding GOME-2 FRESCOv6 cloud top height (upper middle plot) and GOME-2 Absorbing Aerosol Index (upper right plot) for individual days in April and May 2010. Dotted lines indicate area of comparison. The bottom plots show the correlation between SEVIRI-KNMI ash height and GOME-2 FRESCOv6 cloud top height (lower left plot; color coding indicates the corresponding AAI value). The lower middle and right plot shows the mean and root-mean-square SEVIRI ash height corresponding to GOME-2 pixels with AAI values larger than 1 and 3, respectively.

Filename	Date	Time UTC
CAL_LID_L1-ValStage1-V3-01.2010-04-15T03-52-34ZN.hdf	15.04.2010	04:00
CAL_LID_L1-ValStage1-V3-01.2010-04-15T12-53-26ZD.hdf	15.04.2010	13:30
CAL_LID_L1-ValStage1-V3-01.2010-04-16T01-18-07ZN.hdf	16.04.2010	01:15
CAL_LID_L1-ValStage1-V3-01.2010-04-16T10-19-03ZD.hdf	16.04.2010	10:45
CAL_LID_L1-ValStage1-V3-01.2010-04-16T11-57-54ZD.hdf	16.04.2010	12:30
CAL_LID_L1-ValStage1-V3-01.2010-04-17T02-47-56ZD.hdf	17.04.2010	02:15
CAL_LID_L1-ValStage1-V3-01.2010-04-17T03-40-21ZN.hdf	17.04.2010	03:45
CAL_LID_L1-ValStage1-V3-01.2010-04-17T11-02-22ZD.hdf	17.04.2010	13:00
CAL_LID_L1-ValStage1-V3-01.2010-04-20T04-11-30ZN.hdf	20.04.2010	04:15
CAL_LID_L1-ValStage1-V3-01.2010-04-20T13-12-27ZD.hdf	20.04.2010	13:45
CAL_LID_L1-ValStage1-V3-01.2010-04-24T03-47-03ZN.hdf	24.04.2010	04:00
CAL_LID_L1-ValStage1-V3-01.2010-05-06T13-13-42ZD.hdf	06.05.2010	13:45
CAL_LID_L1-ValStage1-V3-01.2010-05-07T03-17-14ZN.hdf	07.05.2010	03:15
CAL_LID_L1-ValStage1-V3-01.2010-05-07T13-57-06ZD.hdf	07.05.2010	14:15
CAL_LID_L1-ValStage1-V3-01.2010-05-08T04-00-33ZN.hdf	08.05.2010	04:00
CAL_LID_L1-ValStage1-V3-01.2010-05-08T14-40-24ZD.hdf	08.05.2010	15:00
CAL_LID_L1-ValStage1-V3-01.2010-05-09T04-43-56ZN.hdf	09.05.2010	04:45
CAL_LID_L1-ValStage1-V3-01.2010-05-09T13-44-52ZD.hdf	09.05.2010	14:00
CAL_LID_L1-ValStage1-V3-01.2010-05-10T03-48-24ZN.hdf	10.05.2010	04:00
CAL_LID_L1-ValStage1-V3-01.2010-05-10T12-49-19ZD.hdf	10.05.2010	14:45
CAL_LID_L1-ValStage1-V3-01.2010-05-11T13-32-37ZD.hdf	11.05.2010	13:45
CAL_LID_L1-ValStage1-V3-01.2010-05-12T03-36-09ZN.hdf	12.05.2010	03:45
CAL_LID_L1-ValStage1-V3-01.2010-05-13T13-20-24ZD.hdf	13.05.2010	13:45
CAL_LID_L1-ValStage1-V3-01.2010-05-14T02-31-31ZD.hdf	14.05.2010	03:15
CAL_LID_L1-ValStage1-V3-01.2010-05-14T12-24-52ZD.hdf	14.05.2010	12:45
CAL_LID_L1-ValStage1-V3-01.2010-05-14T14-03-47ZD.hdf	14.05.2010	14:30
CAL_LID_L1-ValStage1-V3-01.2010-05-15T02-28-24ZN.hdf	15.05.2010	02:45
CAL_LID_L1-ValStage1-V3-01.2010-05-15T04-07-14ZN.hdf	15.05.2010	04:15
CAL_LID_L1-ValStage1-V3-01.2010-05-15T13-08-10ZD.hdf	15.05.2010	13:45
CAL_LID_L1-ValStage1-V3-01.2010-05-16T03-11-42ZN.hdf	16.05.2010	03:15
CAL_LID_L1-ValStage1-V3-01.2010-05-16T03-58-12ZD.hdf	16.05.2010	04:45
CAL_LID_L1-ValStage1-V3-01.2010-05-16T12-12-38ZD.hdf	16.05.2010	12:45
CAL_LID_L1-ValStage1-V3-01.2010-05-16T13-51-28ZD.hdf	16.05.2010	14:00
CAL_LID_L1-ValStage1-V3-01.2010-05-17T02-16-05ZN.hdf	17.05.2010	02:15
CAL_LID_L1-ValStage1-V3-01.2010-05-17T03-55-00ZN.hdf	17.05.2010	04:00
CAL_LID_L1-ValStage1-V3-01.2010-05-17T12-55-56ZD.hdf	17.05.2010	13:15
CAL_LID_L1-ValStage1-V3-01.2010-05-18T02-59-28ZN.hdf	18.05.2010	03:15
CAL_LID_L1-ValStage1-V3-01.2010-05-18T04-38-19ZN.hdf	18.05.2010	04:30
CAL_LID_L1-ValStage1-V3-01.2010-05-18T12-00-25ZD.hdf	18.05.2010	12:35

Table S1

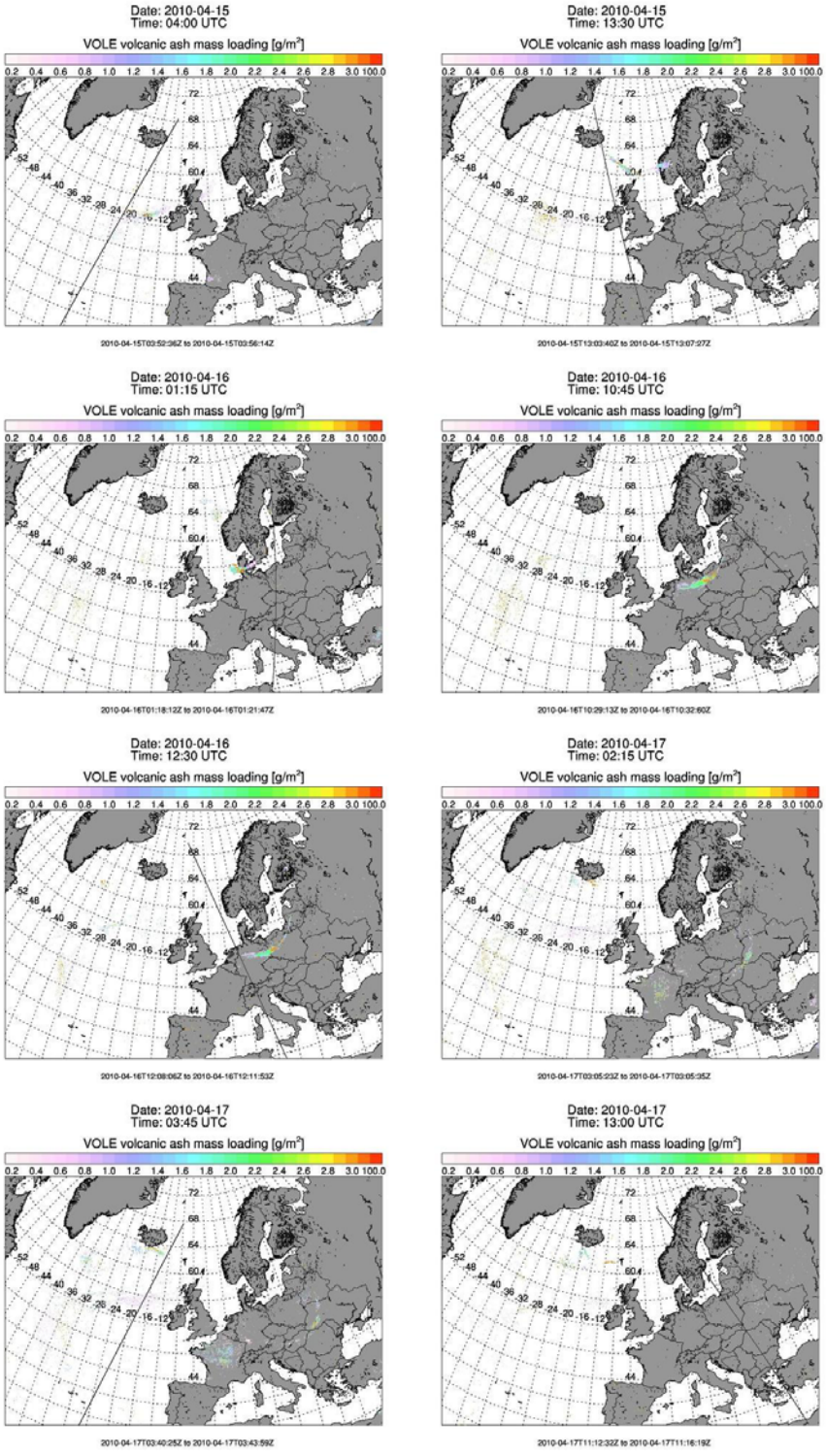
Date: 2010-04-15
Time: 04:00 UTC
VOLE volcanic ash mass loading [g/m²]
Date: 2010-04-15
Time: 13:30 UTC
VOLE volcanic ash mass loading [g/m²]
Date: 2010-04-16
Time: 01:15 UTC
VOLE volcanic ash mass loading [g/m²]
Date: 2010-04-16
Time: 10:45 UTC
VOLE volcanic ash mass loading [g/m²]
Date: 2010-04-16
Time: 12:30 UTC
VOLE volcanic ash mass loading [g/m²]
Date: 2010-04-17
Time: 02:15 UTC
VOLE volcanic ash mass loading [g/m²]
Date: 2010-04-17
Time: 03:45 UTC
VOLE volcanic ash mass loading [g/m²]
Date: 2010-04-17
Time: 13:00 UTC
VOLE volcanic ash mass loading [g/m²]

FigureS1-01.

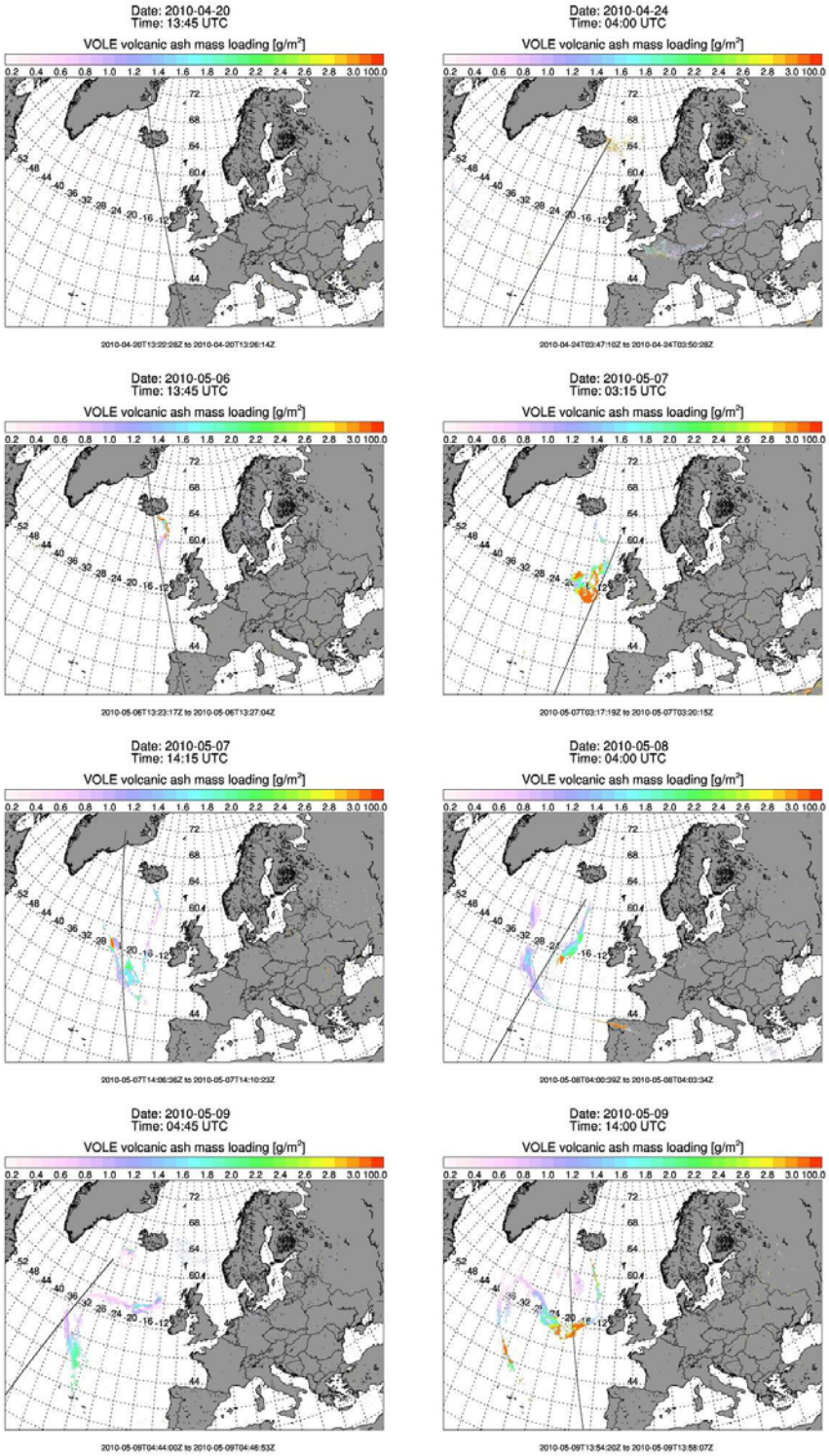
Date: 2010-04-20
Time: 13:45 UTC
VOLE volcanic ash mass loading [g/m²]
Date: 2010-04-24
Time: 04:00 UTC
VOLE volcanic ash mass loading [g/m²]
Date: 2010-05-06
Time: 13:45 UTC
VOLE volcanic ash mass loading [g/m²]
Date: 2010-05-07
Time: 03:15 UTC
VOLE volcanic ash mass loading [g/m²]
Date: 2010-05-07
Time: 14:15 UTC
VOLE volcanic ash mass loading [g/m²]
Date: 2010-05-08
Time: 04:00 UTC
VOLE volcanic ash mass loading [g/m²]
Date: 2010-05-09
Time: 04:45 UTC
VOLE volcanic ash mass loading [g/m²]
Date: 2010-05-09
Time: 14:00 UTC
VOLE volcanic ash mass loading [g/m²]

Figure S1-02.

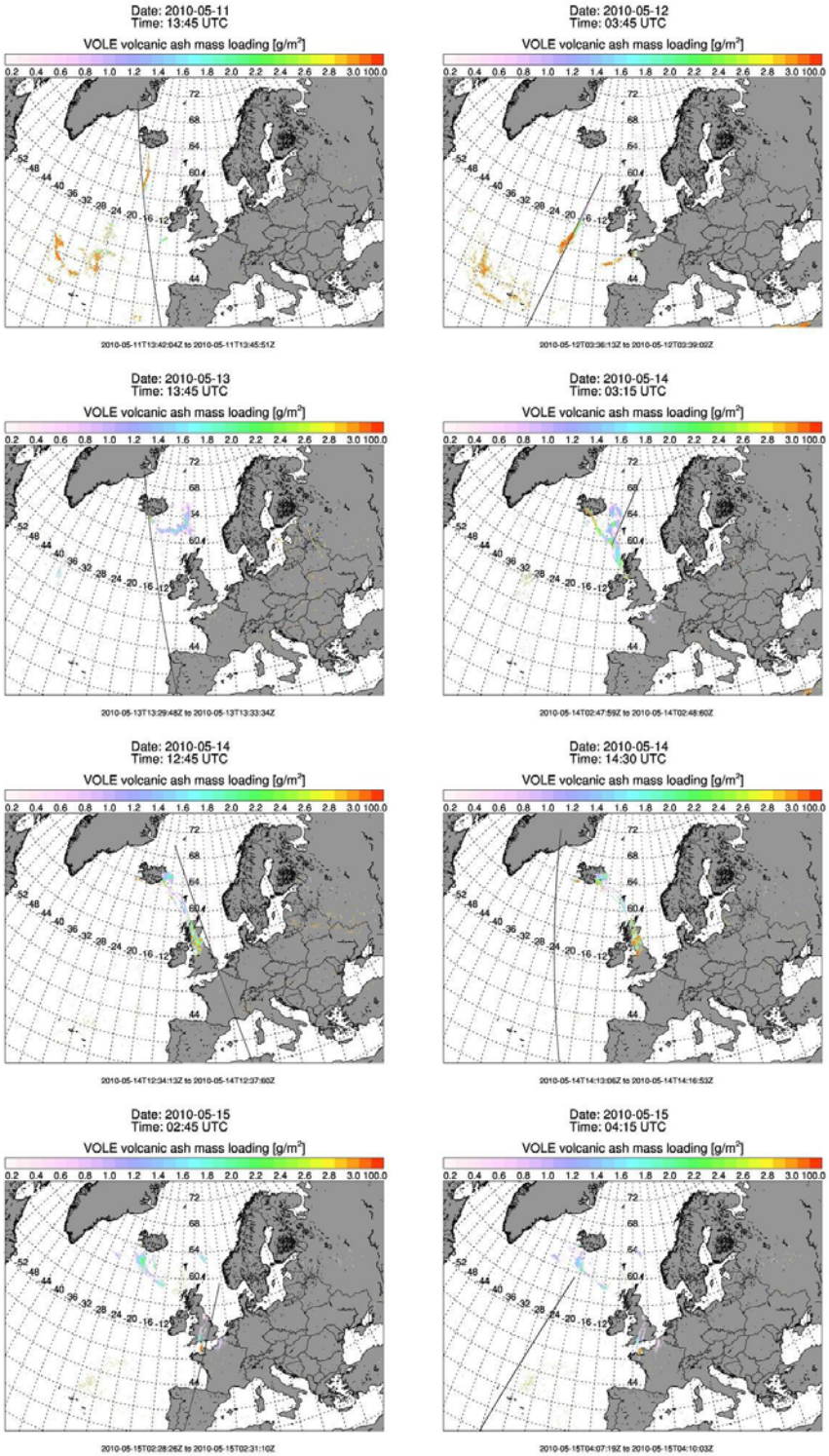
Date: 2010-05-11
Time: 13:45 UTC
VOLE volcanic ash mass loading [g/m²]
Date: 2010-05-12
Time: 03:45 UTC
VOLE volcanic ash mass loading [g/m²]
Date: 2010-05-13
Time: 13:45 UTC
VOLE volcanic ash mass loading [g/m²]
Date: 2010-05-14
Time: 03:15 UTC
VOLE volcanic ash mass loading [g/m²]
Date: 2010-05-14
Time: 12:45 UTC
VOLE volcanic ash mass loading [g/m²]
Date: 2010-05-14
Time: 14:30 UTC
VOLE volcanic ash mass loading [g/m²]
Date: 2010-05-15
Time: 02:45 UTC
VOLE volcanic ash mass loading [g/m²]
Date: 2010-05-15
Time: 04:15 UTC
VOLE volcanic ash mass loading [g/m²]

Figure S1-03.

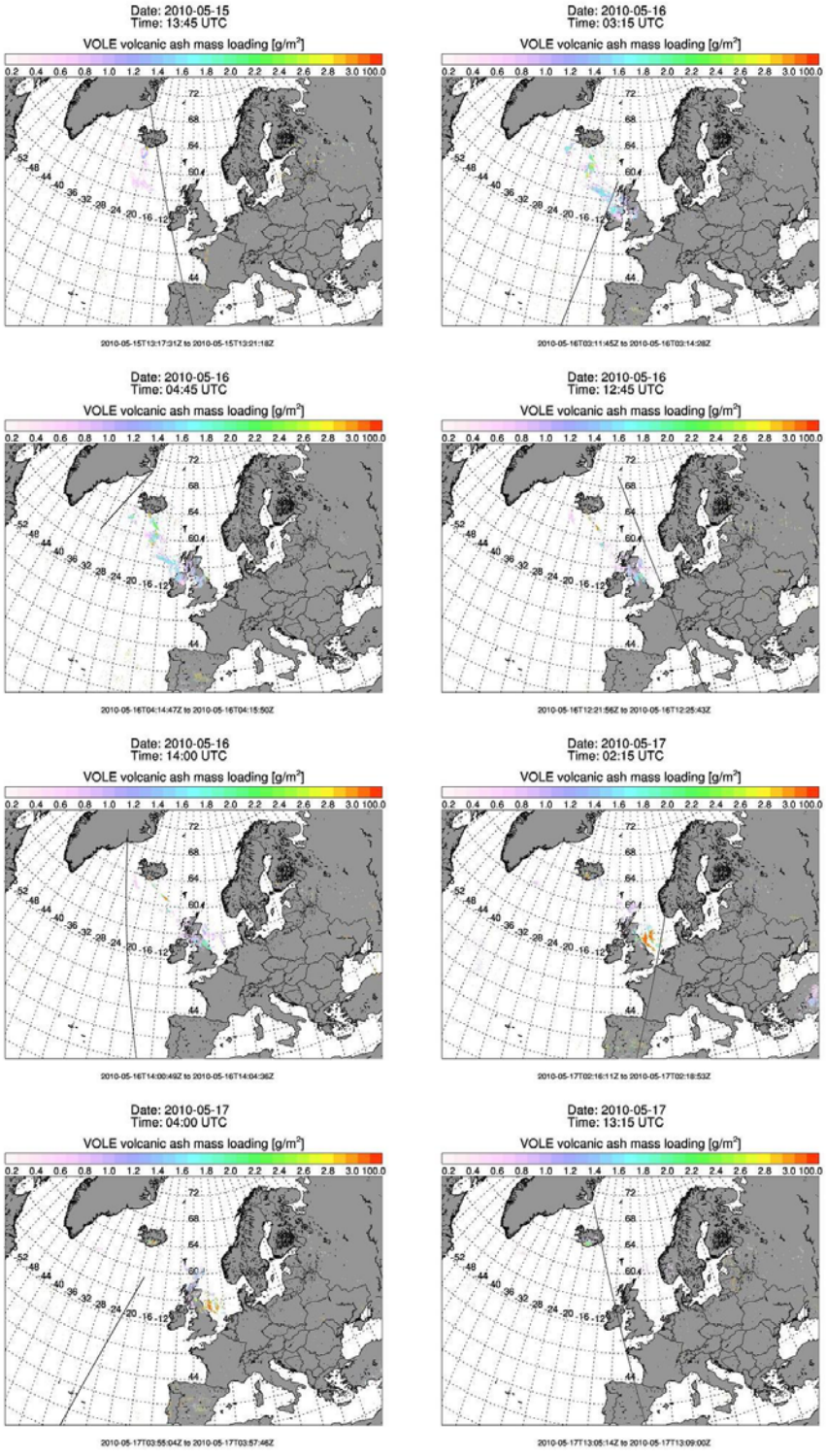
Date: 2010-05-15
Time: 13:45 UTC
VOLE volcanic ash mass loading [g/m²]
Date: 2010-05-16
Time: 03:15 UTC
VOLE volcanic ash mass loading [g/m²]
Date: 2010-05-16
Time: 04:45 UTC
VOLE volcanic ash mass loading [g/m²]
Date: 2010-05-16
Time: 12:45 UTC
VOLE volcanic ash mass loading [g/m²]
Date: 2010-05-16
Time: 14:00 UTC
VOLE volcanic ash mass loading [g/m²]
Date: 2010-05-17
Time: 02:15 UTC
VOLE volcanic ash mass loading [g/m²]
Date: 2010-05-17
Time: 04:00 UTC
VOLE volcanic ash mass loading [g/m²]
Date: 2010-05-17
Time: 13:15 UTC
VOLE volcanic ash mass loading [g/m²]

Figure S1-04.

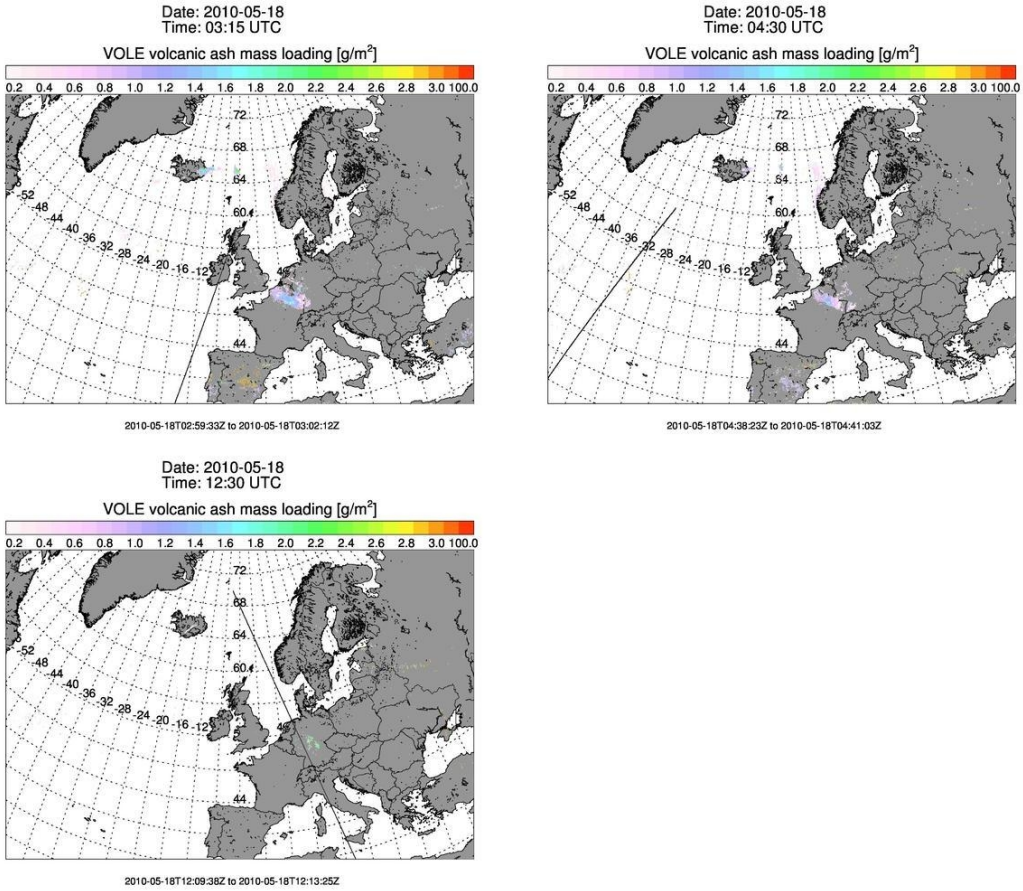
Date: 2010-05-18
Time: 03:15 UTC
VOLE volcanic ash mass loading [g/m²]
0.2 0.4 0.6 0.8 1.0 1.2 1.4 1.6 1.8 2.0 2.2 2.4 2.6 2.8 3.0 100.0
2010-05-18T02:59:33Z to 2010-05-18T03:02:12Z
Date: 2010-05-18
Time: 04:30 UTC
VOLE volcanic ash mass loading [g/m²]
0.2 0.4 0.6 0.8 1.0 1.2 1.4 1.6 1.8 2.0 2.2 2.4 2.6 2.8 3.0 100.0
2010-05-18T04:38:23Z to 2010-05-18T04:41:03Z
Date: 2010-05-18
Time: 12:30 UTC
VOLE volcanic ash mass loading [g/m²]
0.2 0.4 0.6 0.8 1.0 1.2 1.4 1.6 1.8 2.0 2.2 2.4 2.6 2.8 3.0 100.0
2010-05-18T12:09:38Z to 2010-05-18T12:13:25Z

Figure S1-05.

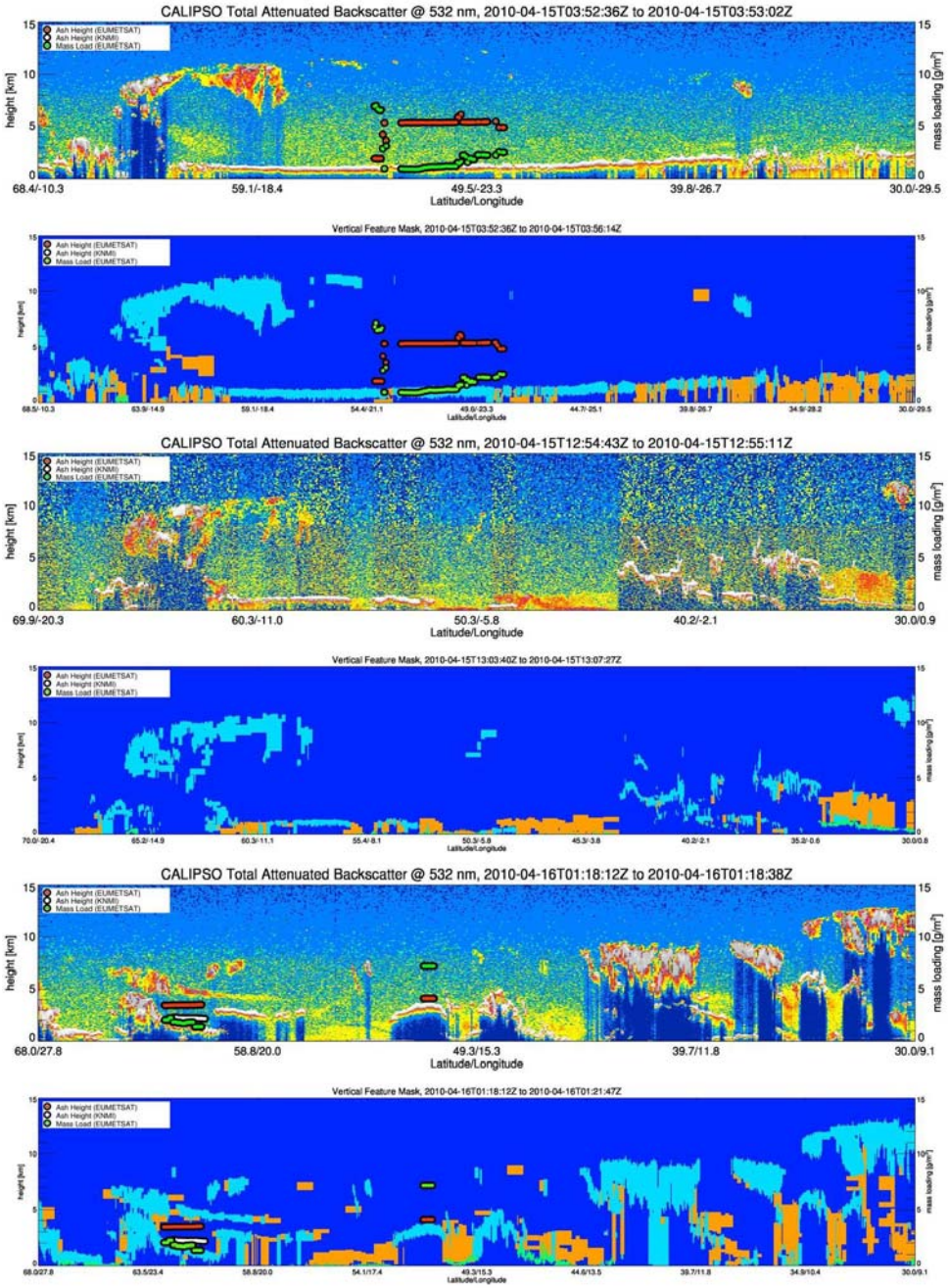
CALIPSO Total Attenuated Backscatter @ 532 nm, 2010-04-15T03:52:36Z to 2010-04-15T03:53:02Z
Ash Height (EUMETSAT)
Ash Height (KNMI)
Mass Load (EUMETSAT)
height [km]
mass loading [g/m²]
68.4/-10.3
59.1/-18.4
49.5/-23.3
39.8/-26.7
30.0/-29.5
Latitude/Longitude
Vertical Feature Mask, 2010-04-15T03:52:36Z to 2010-04-15T03:56:14Z
CALIPSO Total Attenuated Backscatter @ 532 nm, 2010-04-15T12:54:43Z to 2010-04-15T12:55:11Z
69.9/-20.3
60.3/-11.0
50.3/-5.8
40.2/-2.1
30.0/0.9
Vertical Feature Mask, 2010-04-15T13:03:40Z to 2010-04-15T13:07:27Z
CALIPSO Total Attenuated Backscatter @ 532 nm, 2010-04-16T01:18:12Z to 2010-04-16T01:18:38Z
68.0/27.8
58.8/20.0
49.3/15.3
39.7/11.8
30.0/9.1
Vertical Feature Mask, 2010-04-16T01:18:12Z to 2010-04-16T01:21:47Z

Figure S2-01.

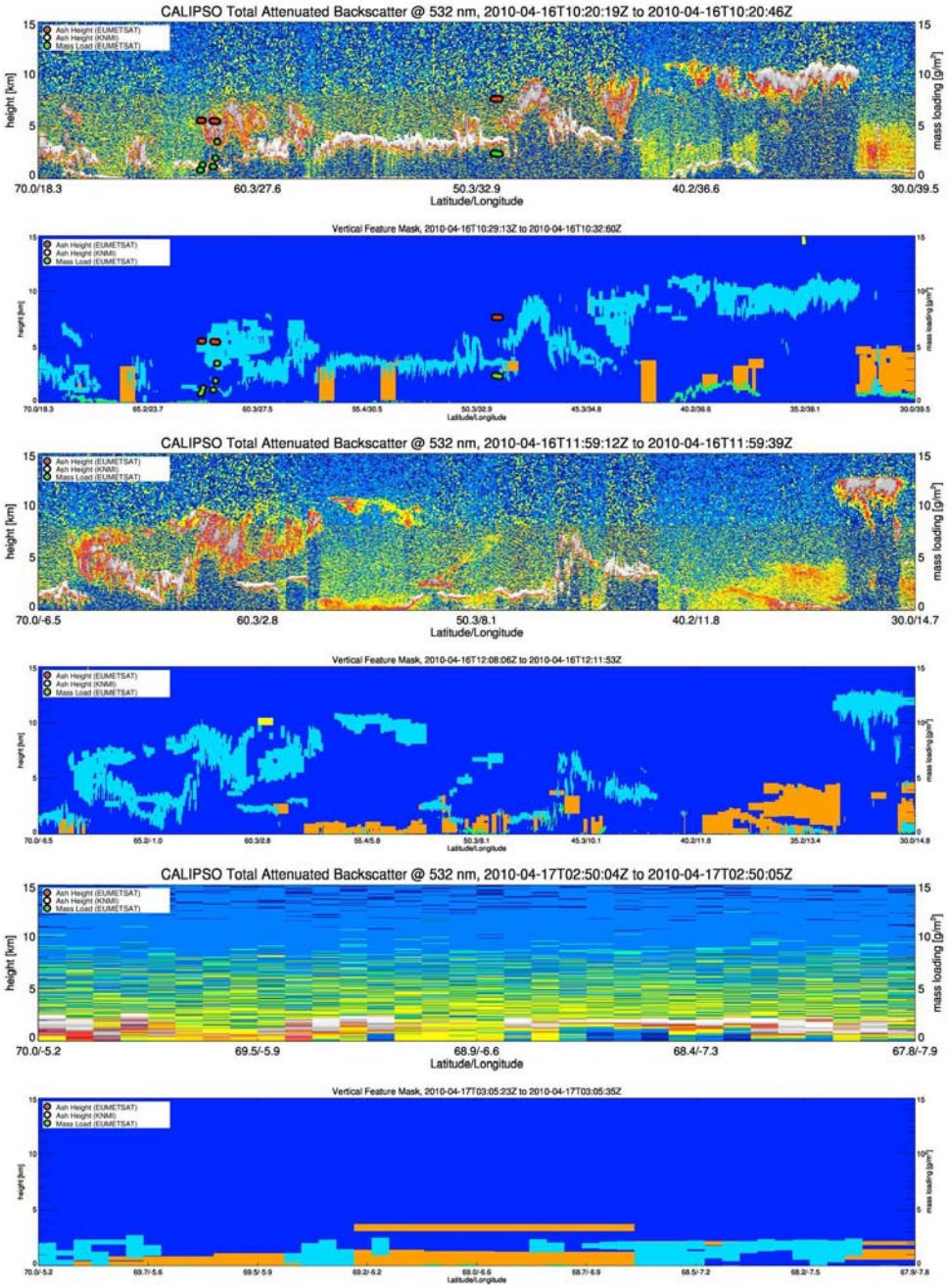
CALIPSO Total Attenuated Backscatter @ 532 nm, 2010-04-16T10:20:19Z to 2010-04-16T10:20:46Z
Ash Height (EUMETSAT)
Ash Height (KNMI)
Mass Load (EUMETSAT)
height [km]
mass loading [g/m²]
70.0/18.3
60.3/27.6
50.3/32.9
40.2/36.6
30.0/39.5
Latitude/Longitude
Vertical Feature Mask, 2010-04-16T10:29:13Z to 2010-04-16T10:32:60Z
CALIPSO Total Attenuated Backscatter @ 532 nm, 2010-04-16T11:59:12Z to 2010-04-16T11:59:39Z
70.0/-6.5
60.3/2.8
50.3/8.1
40.2/11.8
30.0/14.7
Vertical Feature Mask, 2010-04-16T12:08:06Z to 2010-04-16T12:11:53Z
CALIPSO Total Attenuated Backscatter @ 532 nm, 2010-04-17T02:50:04Z to 2010-04-17T02:50:05Z
70.0/-5.2
69.5/-5.9
68.9/-6.6
68.4/-7.3
67.8/-7.9
Vertical Feature Mask, 2010-04-17T03:05:23Z to 2010-04-17T03:05:35Z

Figure S2-02.

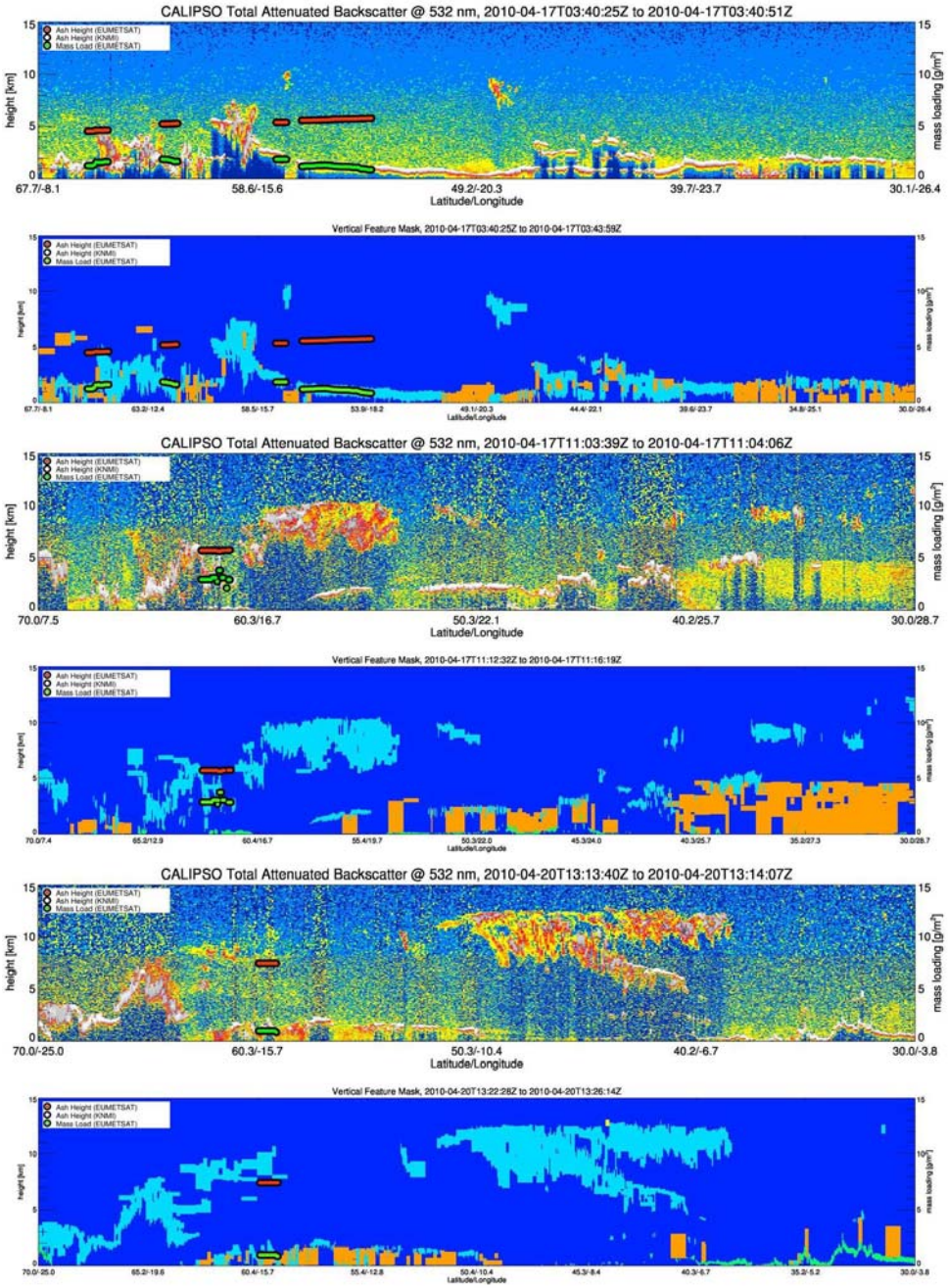
CALIPSO Total Attenuated Backscatter @ 532 nm, 2010-04-17T03:40:25Z to 2010-04-17T03:40:51Z
Ash Height (EUMETSAT)
Ash Height (KNMI)
Mass Load (EUMETSAT)
height [km]
mass loading [g/m²]
67.7/-8.1
58.6/-15.6
49.2/-20.3
39.7/-23.7
30.1/-26.4
Latitude/Longitude
Vertical Feature Mask, 2010-04-17T03:40:25Z to 2010-04-17T03:43:59Z
CALIPSO Total Attenuated Backscatter @ 532 nm, 2010-04-17T11:03:39Z to 2010-04-17T11:04:06Z
70.0/7.5
60.3/16.7
50.3/22.1
40.2/25.7
30.0/28.7
Vertical Feature Mask, 2010-04-17T11:12:32Z to 2010-04-17T11:16:19Z
CALIPSO Total Attenuated Backscatter @ 532 nm, 2010-04-20T13:13:40Z to 2010-04-20T13:14:07Z
70.0/-25.0
60.3/-15.7
50.3/-10.4
40.2/-6.7
30.0/-3.8
Vertical Feature Mask, 2010-04-20T13:22:28Z to 2010-04-20T13:26:14Z

Figure S2-.03.

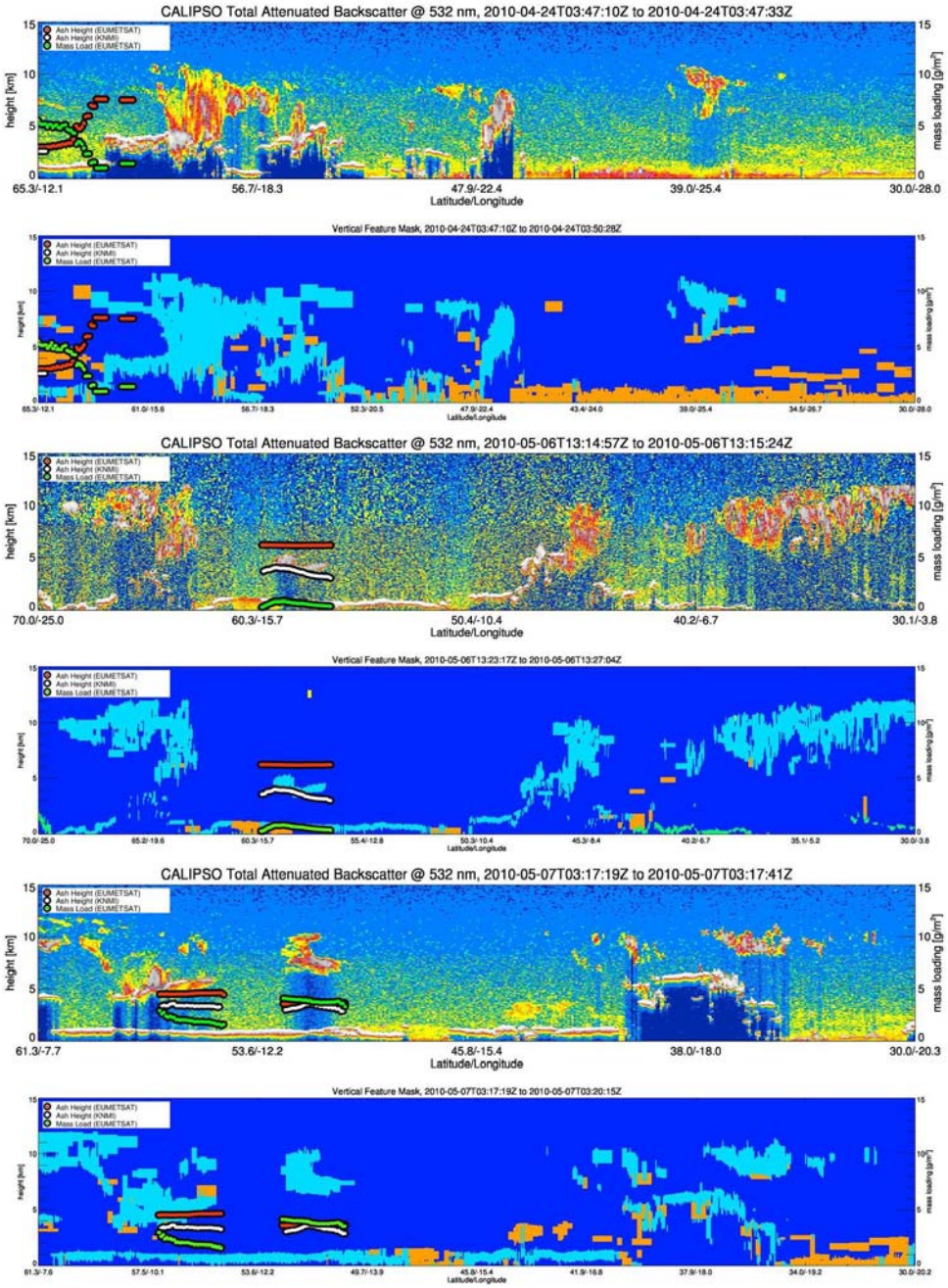
CALIPSO Total Attenuated Backscatter @ 532 nm, 2010-04-24T03:47:10Z to 2010-04-24T03:47:33Z
Ash Height (EUMETSAT)
Ash Height (KNMI)
Mass Load (EUMETSAT)
height [km]
mass loading [g/m²]
65.3/-12.1
56.7/-18.3
47.9/-22.4
39.0/-25.4
30.0/-28.0
Latitude/Longitude
Vertical Feature Mask, 2010-04-24T03:47:10Z to 2010-04-24T03:50:28Z
CALIPSO Total Attenuated Backscatter @ 532 nm, 2010-05-06T13:14:57Z to 2010-05-06T13:15:24Z
70.0/-25.0
60.3/-15.7
50.4/-10.4
40.2/-6.7
30.1/-3.8
Vertical Feature Mask, 2010-05-06T13:23:17Z to 2010-05-06T13:27:04Z
CALIPSO Total Attenuated Backscatter @ 532 nm, 2010-05-07T03:17:19Z to 2010-05-07T03:17:41Z
61.3/-7.7
53.6/-12.2
45.8/-15.4
38.0/-18.0
30.0/-20.3
Vertical Feature Mask, 2010-05-07T03:17:19Z to 2010-05-07T03:20:15Z

Figure S2-04.

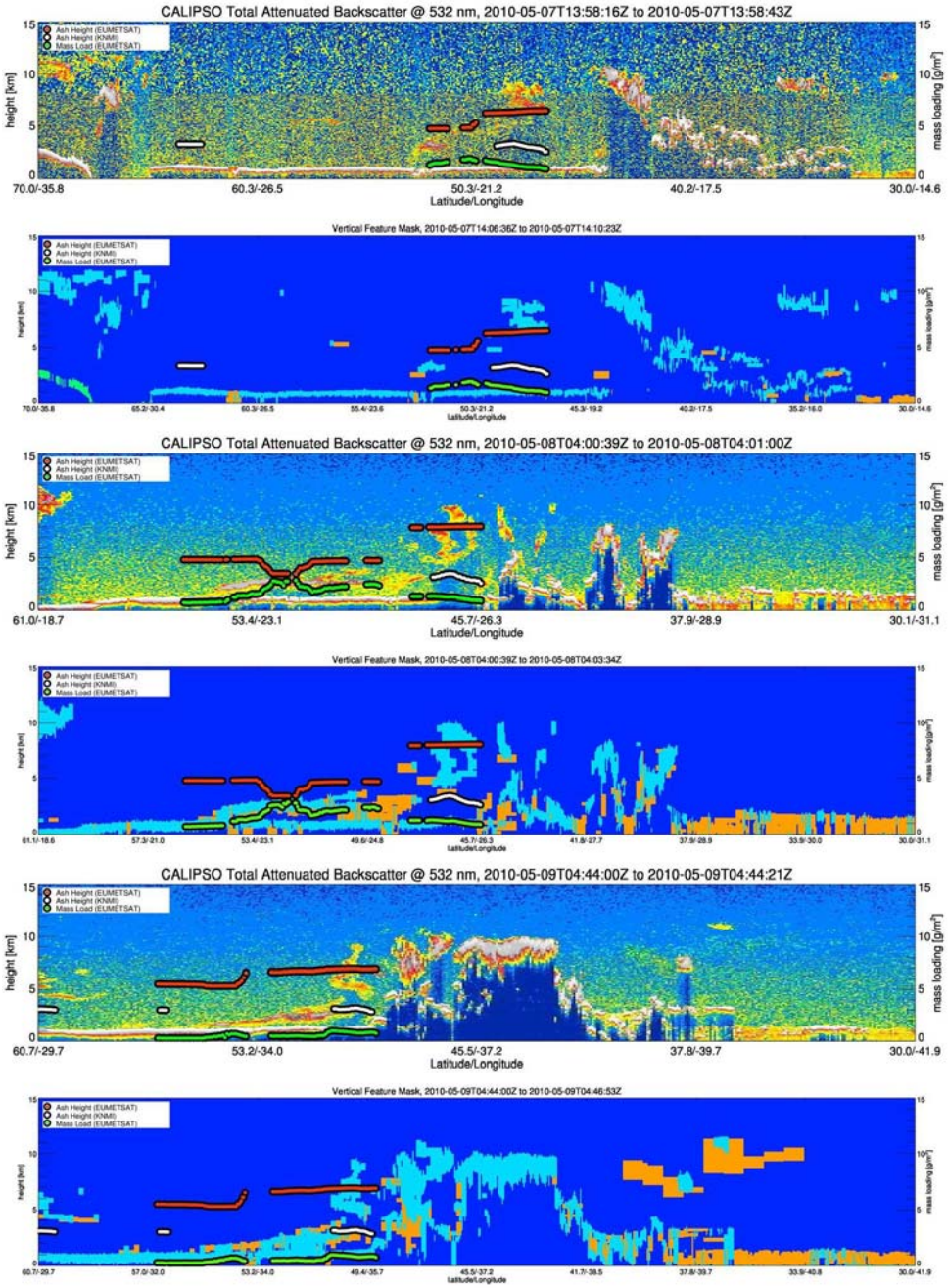
CALIPSO Total Attenuated Backscatter @ 532 nm, 2010-05-07T13:58:16Z to 2010-05-07T13:58:43Z
Ash Height (EUMETSAT)
Ash Height (KNMI)
Mass Load (EUMETSAT)
height [km]
mass loading [g/m²]
70.0/-35.8
60.3/-26.5
50.3/-21.2
40.2/-17.5
30.0/-14.6
Latitude/Longitude
Vertical Feature Mask, 2010-05-07T14:06:36Z to 2010-05-07T14:10:23Z
CALIPSO Total Attenuated Backscatter @ 532 nm, 2010-05-08T04:00:39Z to 2010-05-08T04:01:00Z
61.0/-18.7
53.4/-23.1
45.7/-26.3
37.9/-28.9
30.1/-31.1
Vertical Feature Mask, 2010-05-08T04:00:39Z to 2010-05-08T04:03:34Z
CALIPSO Total Attenuated Backscatter @ 532 nm, 2010-05-09T04:44:00Z to 2010-05-09T04:44:21Z
60.7/-29.7
53.2/-34.0
45.5/-37.2
37.8/-39.7
30.0/-41.9
Vertical Feature Mask, 2010-05-09T04:44:00Z to 2010-05-09T04:46:53Z

Figure S2-05.

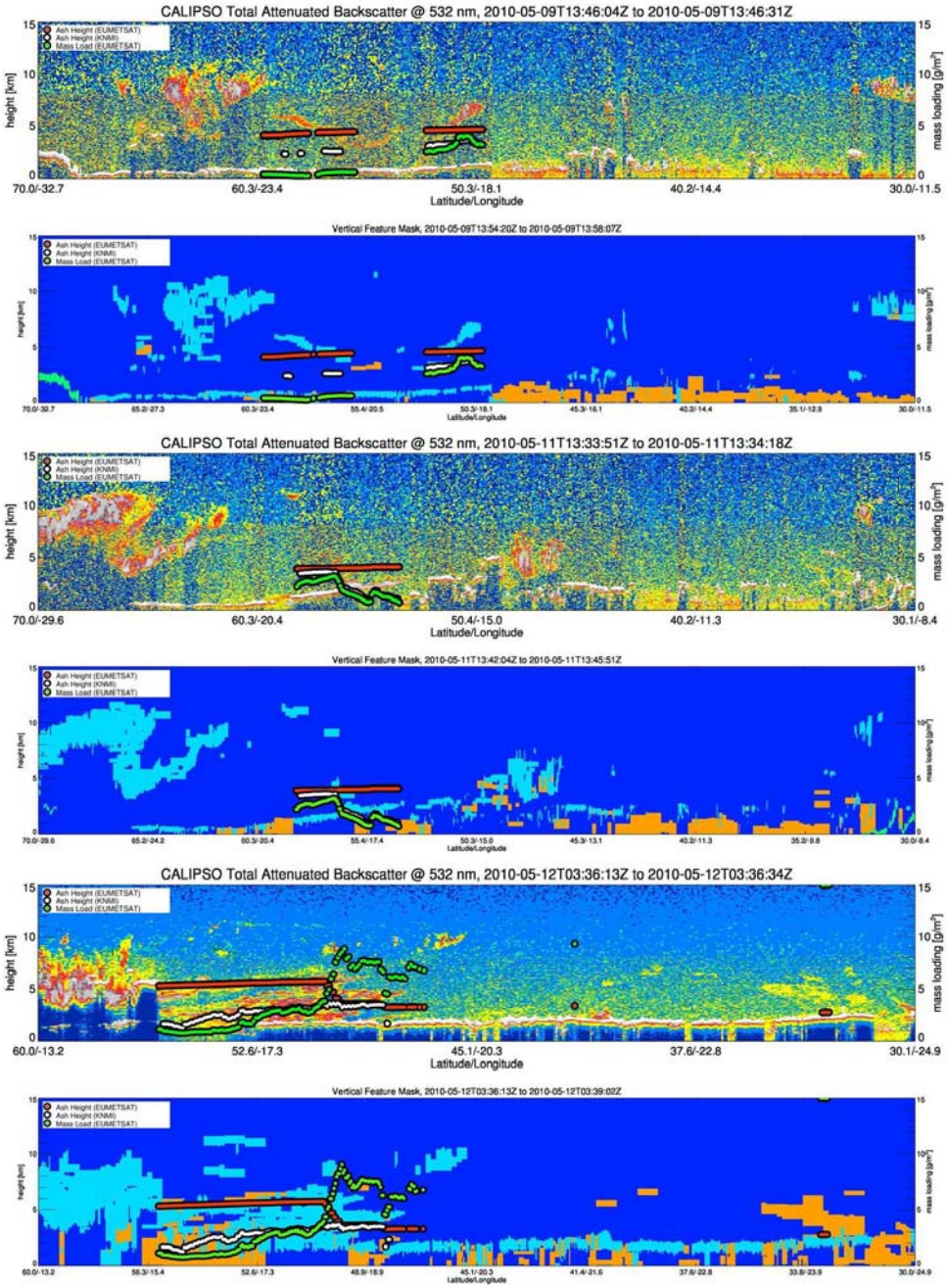
CALIPSO Total Attenuated Backscatter @ 532 nm, 2010-05-09T13:46:04Z to 2010-05-09T13:46:31Z
Ash Height (EUMETSAT)
Ash Height (KNMI)
Mass Load (EUMETSAT)
height [km]
mass loading [g/m²]
70.0/-32.7
60.3/-23.4
50.3/-18.1
40.2/-14.4
30.0/-11.5
Latitude/Longitude
Vertical Feature Mask, 2010-05-09T13:54:20Z to 2010-05-09T13:58:07Z
CALIPSO Total Attenuated Backscatter @ 532 nm, 2010-05-11T13:33:51Z to 2010-05-11T13:34:18Z
70.0/-29.6
60.3/-20.4
50.4/-15.0
40.2/-11.3
30.1/-8.4
Vertical Feature Mask, 2010-05-11T13:42:04Z to 2010-05-11T13:45:51Z
CALIPSO Total Attenuated Backscatter @ 532 nm, 2010-05-12T03:36:13Z to 2010-05-12T03:36:34Z
60.0/-13.2
52.6/-17.3
45.1/-20.3
37.6/-22.8
30.1/-24.9
Vertical Feature Mask, 2010-05-12T03:36:13Z to 2010-05-12T03:39:02Z

Figure S2-06.

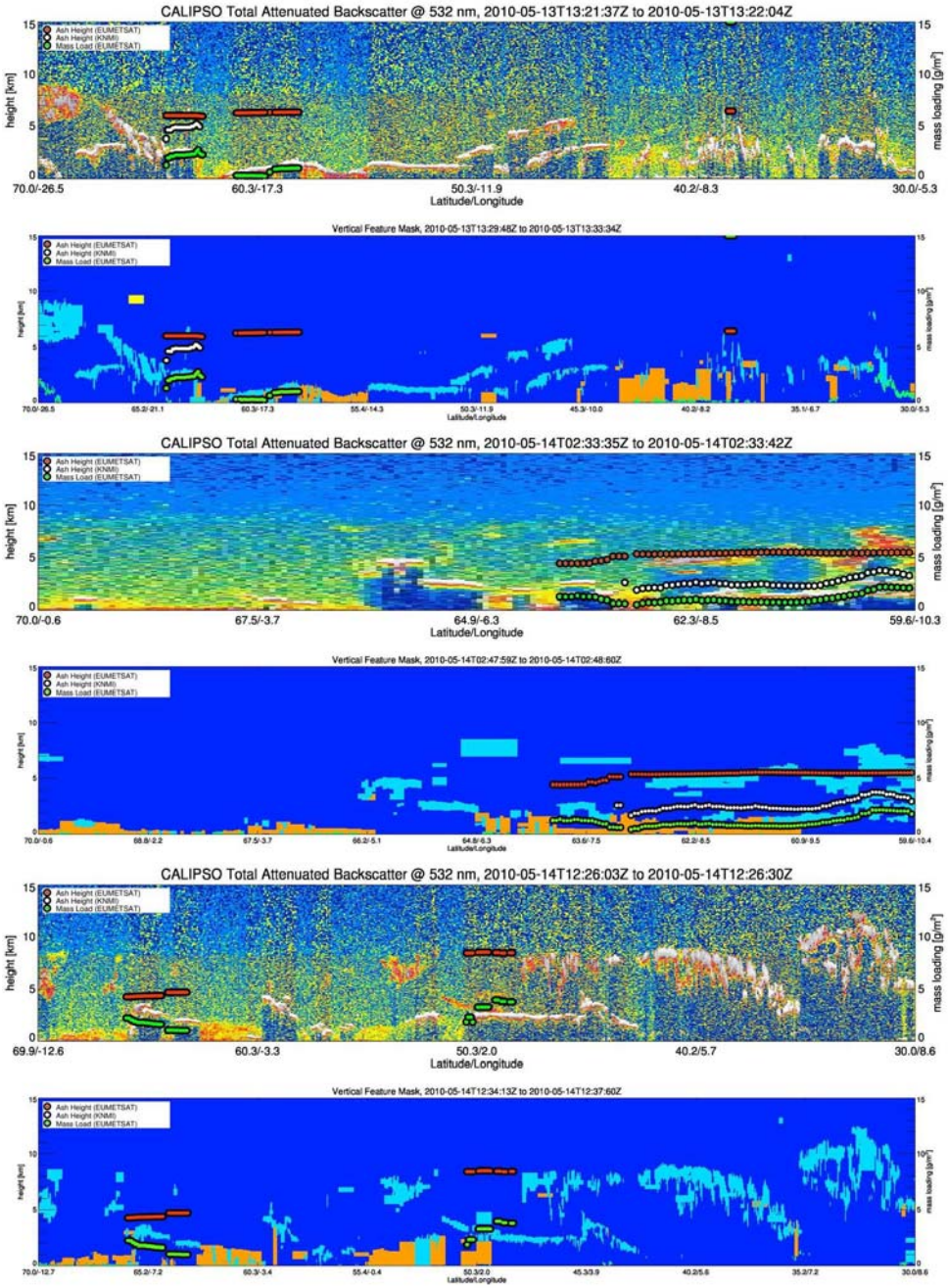
CALIPSO Total Attenuated Backscatter @ 532 nm, 2010-05-13T13:21:37Z to 2010-05-13T13:22:04Z
Ash Height (EUMETSAT)
Ash Height (KNMI)
Mass Load (EUMETSAT)
height [km]
mass loading [g/m²]
70.0/-26.5
60.3/-17.3
50.3/-11.9
40.2/-8.3
30.0/-5.3
Latitude/Longitude
Vertical Feature Mask, 2010-05-13T13:29:48Z to 2010-05-13T13:33:34Z
CALIPSO Total Attenuated Backscatter @ 532 nm, 2010-05-14T02:33:35Z to 2010-05-14T02:33:42Z
70.0/-0.6
67.5/-3.7
64.9/-6.3
62.3/-8.5
59.6/-10.3
Vertical Feature Mask, 2010-05-14T02:47:59Z to 2010-05-14T02:48:60Z
CALIPSO Total Attenuated Backscatter @ 532 nm, 2010-05-14T12:26:03Z to 2010-05-14T12:26:30Z
69.9/-12.6
60.3/-3.3
50.3/2.0
40.2/5.7
30.0/8.6
Vertical Feature Mask, 2010-05-14T12:34:13Z to 2010-05-14T12:37:60Z

Figure S2-07.

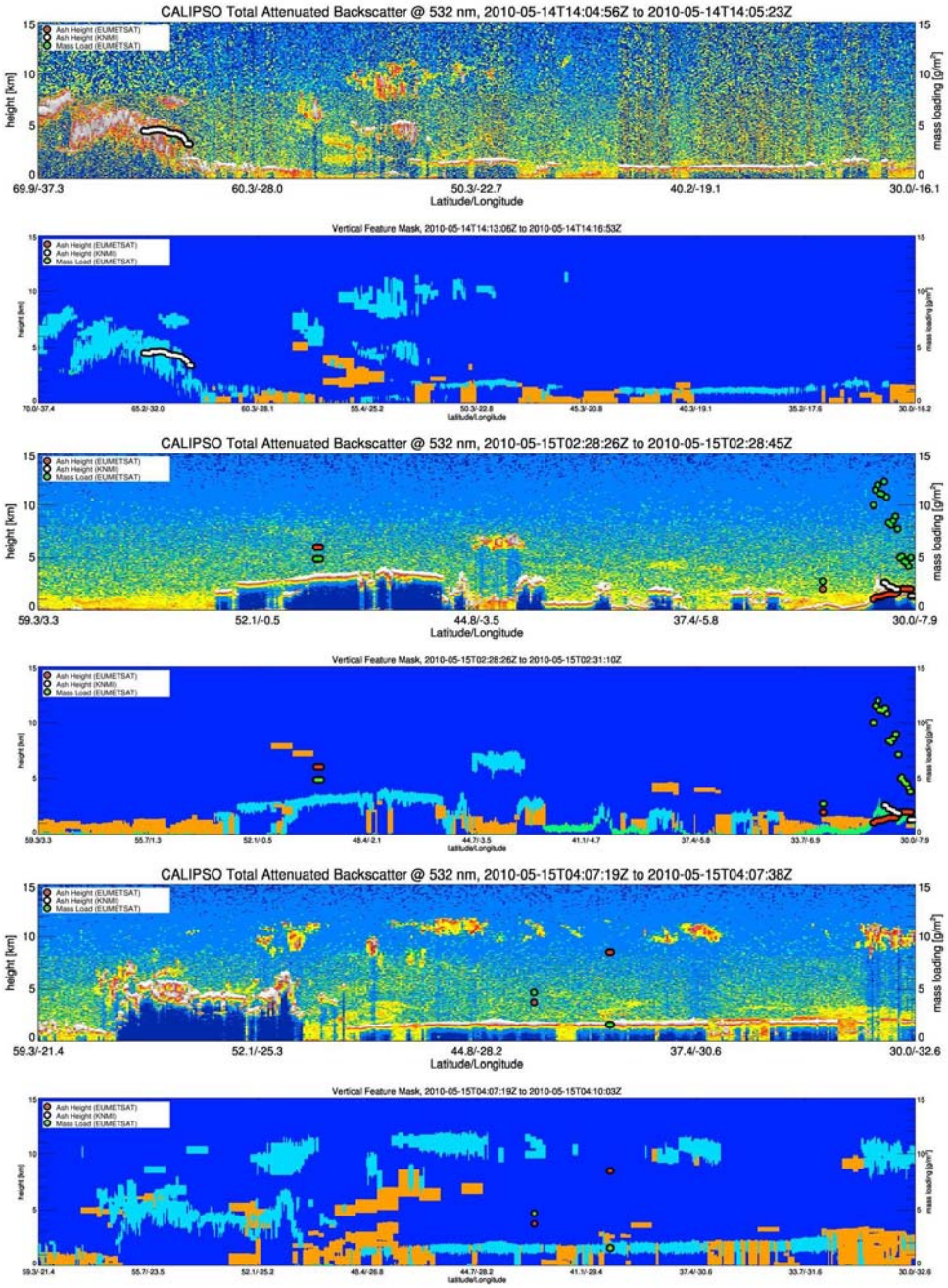
CALIPSO Total Attenuated Backscatter @ 532 nm, 2010-05-14T14:04:56Z to 2010-05-14T14:05:23Z
Ash Height (EUMETSAT)
Ash Height (KNMI)
Mass Load (EUMETSAT)
height [km]
mass loading [g/m²]
69.9/-37.3
60.3/-28.0
50.3/-22.7
40.2/-19.1
30.0/-16.1
Latitude/Longitude
Vertical Feature Mask, 2010-05-14T14:13:06Z to 2010-05-14T14:16:53Z
CALIPSO Total Attenuated Backscatter @ 532 nm, 2010-05-15T02:28:26Z to 2010-05-15T02:28:45Z
59.3/3.3
52.1/-0.5
44.8/-3.5
37.4/-5.8
30.0/-7.9
Vertical Feature Mask, 2010-05-15T02:28:26Z to 2010-05-15T02:31:10Z
CALIPSO Total Attenuated Backscatter @ 532 nm, 2010-05-15T04:07:19Z to 2010-05-15T04:07:38Z
59.3/-21.4
52.1/-25.3
44.8/-28.2
37.4/-30.6
30.0/-32.6
Vertical Feature Mask, 2010-05-15T04:07:19Z to 2010-05-15T04:10:03Z

Figure S2-08.

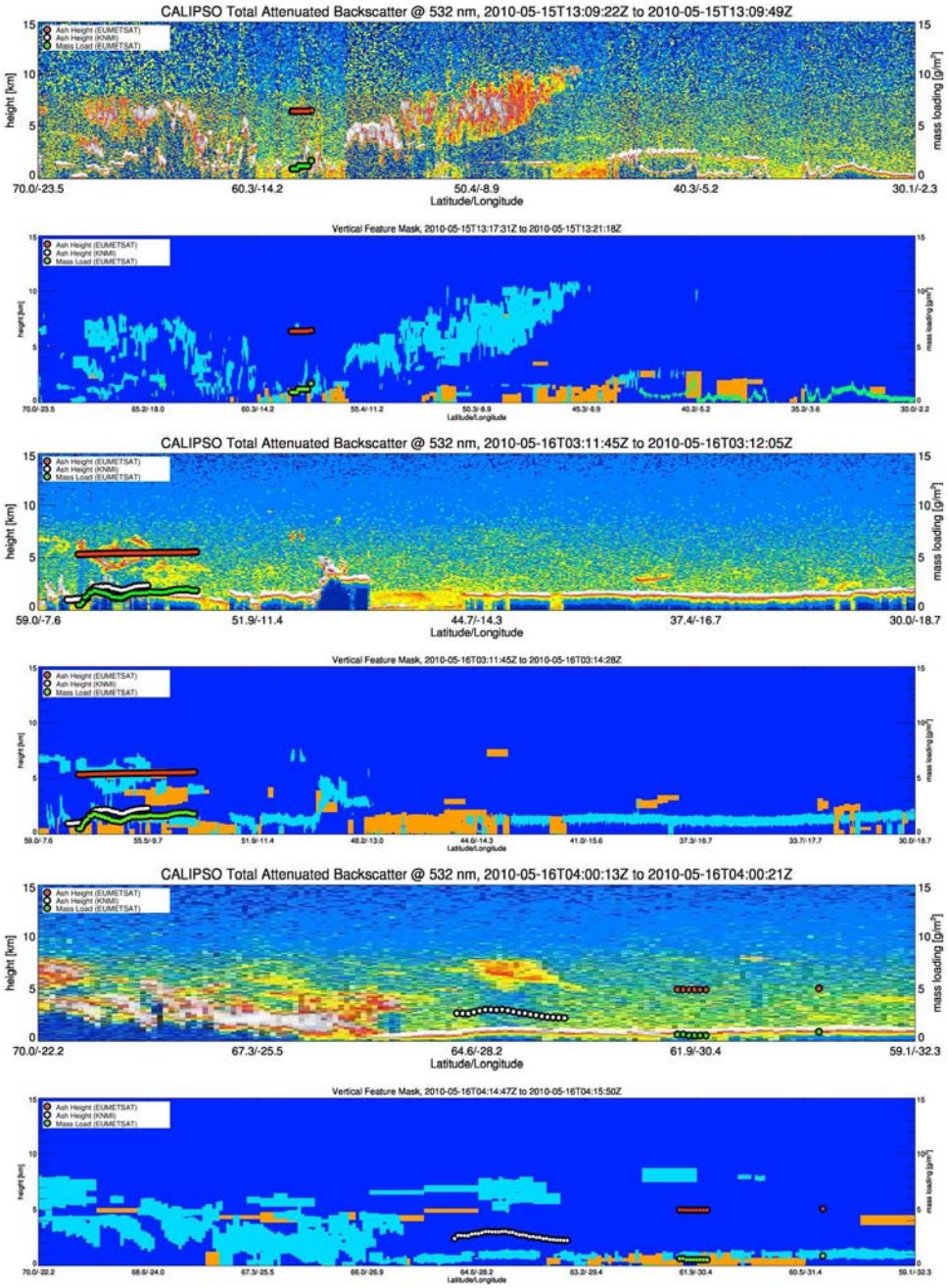
CALIPSO Total Attenuated Backscatter @ 532 nm, 2010-05-15T13:09:22Z to 2010-05-15T13:09:49Z
Ash Height (EUMETSAT)
Ash Height (KNMI)
Mass Load (EUMETSAT)
height [km]
mass loading [g/m²]
70.0/-23.5
60.3/-14.2
50.4/-8.9
40.3/-5.2
30.1/-2.3
Latitude/Longitude
Vertical Feature Mask, 2010-05-15T13:17:31Z to 2010-05-15T13:21:18Z
CALIPSO Total Attenuated Backscatter @ 532 nm, 2010-05-16T03:11:45Z to 2010-05-16T03:12:05Z
59.0/-7.6
51.9/-11.4
44.7/-14.3
37.4/-16.7
30.0/-18.7
Vertical Feature Mask, 2010-05-16T03:11:45Z to 2010-05-16T03:14:28Z
CALIPSO Total Attenuated Backscatter @ 532 nm, 2010-05-16T04:00:13Z to 2010-05-16T04:00:21Z
70.0/-22.2
67.3/-25.5
64.6/-28.2
61.9/-30.4
59.1/-32.3
Vertical Feature Mask, 2010-05-16T04:14:47Z to 2010-05-16T04:15:50Z

Figure S2-09.

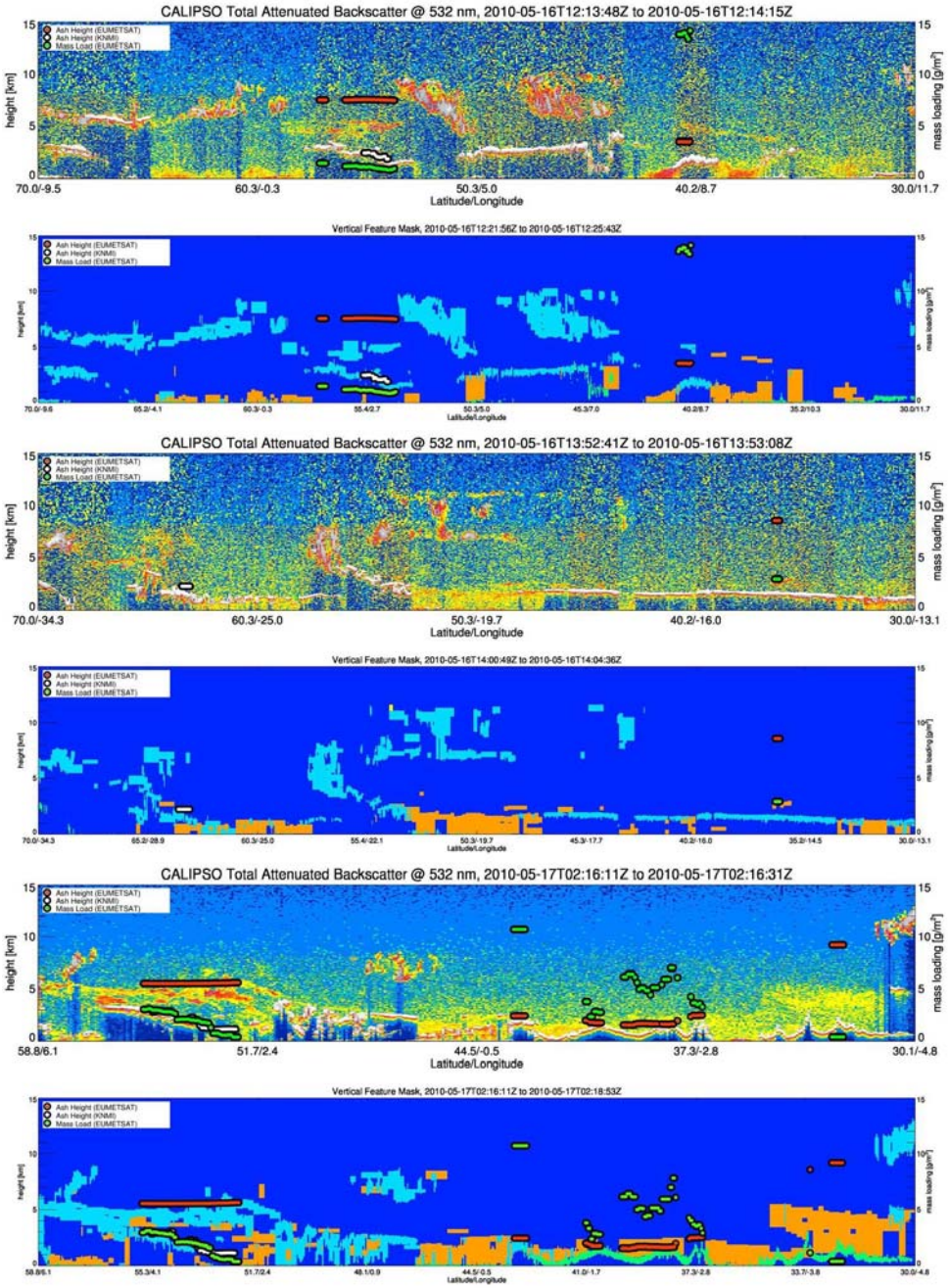
CALIPSO Total Attenuated Backscatter @ 532 nm, 2010-05-16T12:13:48Z to 2010-05-16T12:14:15Z
Ash Height (EUMETSAT)
Ash Height (KNMI)
Mass Load (EUMETSAT)
height [km]
mass loading [g/m²]
70.0/-9.5
60.3/-0.3
50.3/5.0
40.2/8.7
30.0/11.7
Latitude/Longitude
Vertical Feature Mask, 2010-05-16T12:21:56Z to 2010-05-16T12:25:43Z
CALIPSO Total Attenuated Backscatter @ 532 nm, 2010-05-16T13:52:41Z to 2010-05-16T13:53:08Z
70.0/-34.3
60.3/-25.0
50.3/-19.7
40.2/-16.0
30.0/-13.1
Vertical Feature Mask, 2010-05-16T14:00:49Z to 2010-05-16T14:04:36Z
CALIPSO Total Attenuated Backscatter @ 532 nm, 2010-05-17T02:16:11Z to 2010-05-17T02:16:31Z
58.8/6.1
51.7/2.4
44.5/-0.5
37.3/-2.8
30.1/-4.8
Vertical Feature Mask, 2010-05-17T02:16:11Z to 2010-05-17T02:18:53Z

Figure S2-10.

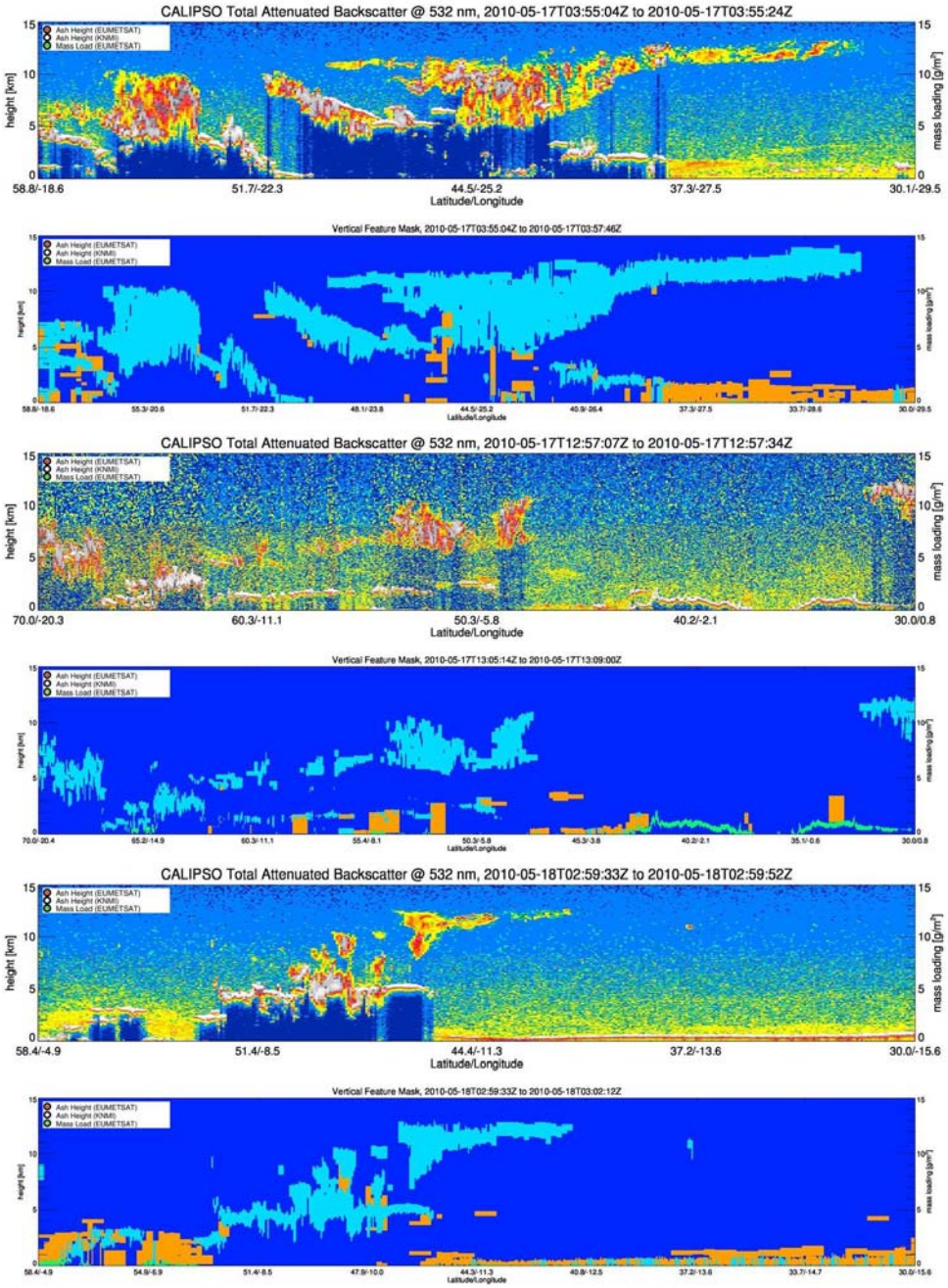
CALIPSO Total Attenuated Backscatter @ 532 nm, 2010-05-17T03:55:04Z to 2010-05-17T03:55:24Z
Ash Height (EUMETSAT)
Ash Height (KNMI)
Mass Load (EUMETSAT)
height [km]
mass loading [g/m²]
58.8/-18.6
51.7/-22.3
44.5/-25.2
37.3/-27.5
30.1/-29.5
Latitude/Longitude
Vertical Feature Mask, 2010-05-17T03:55:04Z to 2010-05-17T03:57:46Z
CALIPSO Total Attenuated Backscatter @ 532 nm, 2010-05-17T12:57:07Z to 2010-05-17T12:57:34Z
70.0/-20.3
60.3/-11.1
50.3/-5.8
40.2/-2.1
30.0/0.8
Vertical Feature Mask, 2010-05-17T13:05:14Z to 2010-05-17T13:09:00Z
CALIPSO Total Attenuated Backscatter @ 532 nm, 2010-05-18T02:59:33Z to 2010-05-18T02:59:52Z
58.4/-4.9
51.4/-8.5
44.4/-11.3
37.2/-13.6
30.0/-15.6
Vertical Feature Mask, 2010-05-18T02:59:33Z to 2010-05-18T03:02:12Z

Figure S2-11.

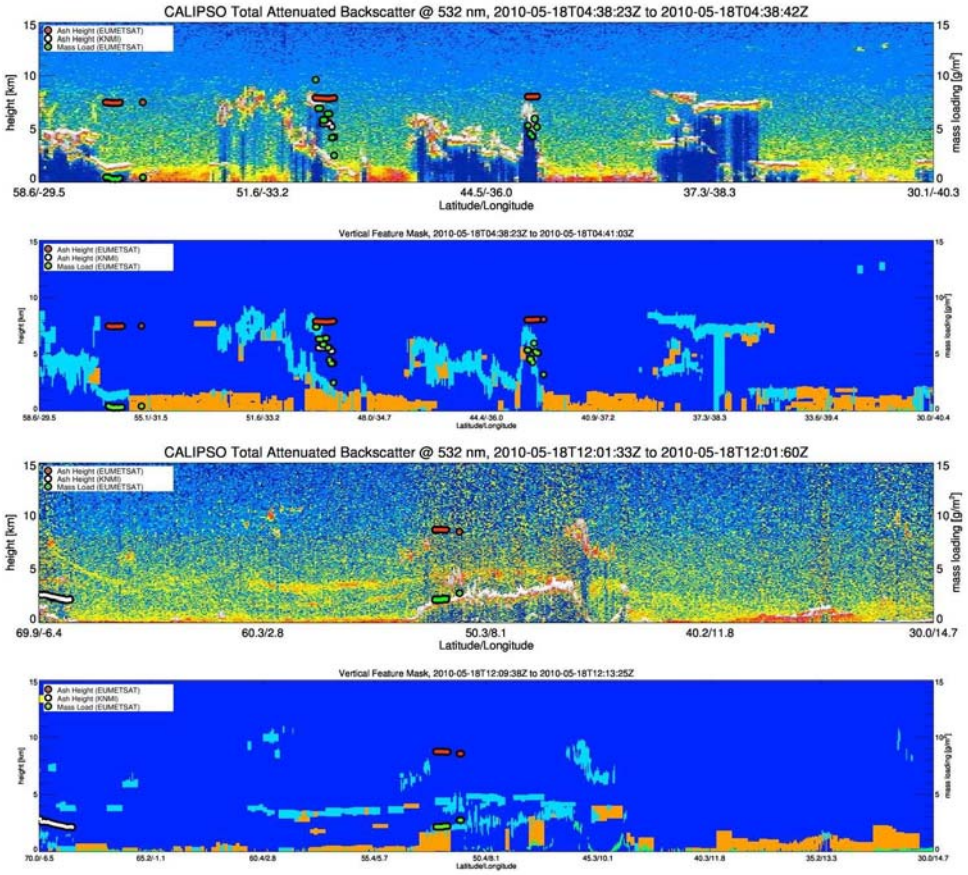
CALIPSO Total Attenuated Backscatter @ 532 nm, 2010-05-18T04:38:23Z to 2010-05-18T04:38:42Z
Ash Height (EUMETSAT)
Ash Height (KNMI)
Mass Load (EUMETSAT)
height [km]
mass loading [g/m²]
58.6/-29.5
51.6/-33.2
44.5/-36.0
37.3/-38.3
30.1/-40.3
Latitude/Longitude
Vertical Feature Mask, 2010-05-18T04:38:23Z to 2010-05-18T04:41:03Z
CALIPSO Total Attenuated Backscatter @ 532 nm, 2010-05-18T12:01:33Z to 2010-05-18T12:01:60Z
69.9/-6.4
60.3/2.8
50.3/8.1
40.2/11.8
30.0/14.7
Vertical Feature Mask, 2010-05-18T12:09:38Z to 2010-05-18T12:13:25Z

Figure S2-12.

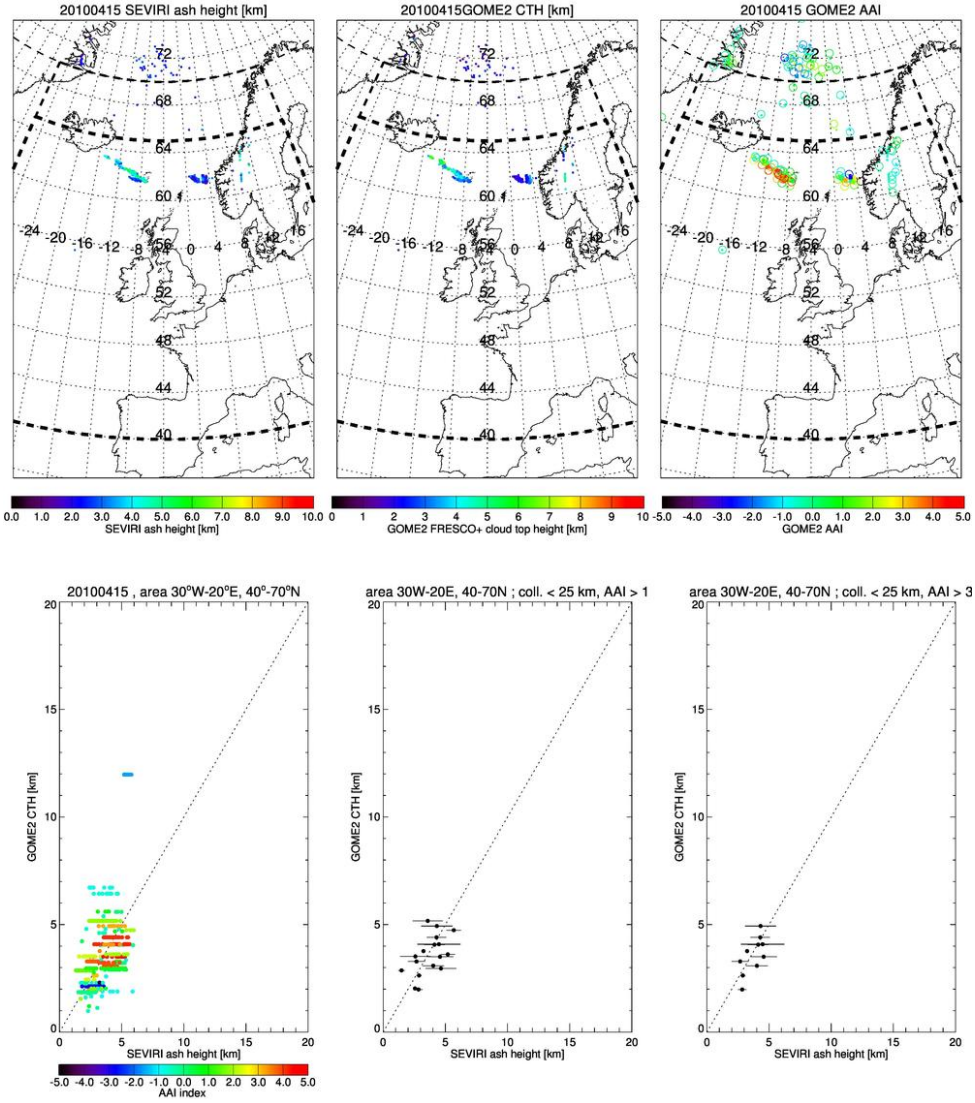

Figure S3-01. 15 April 2010

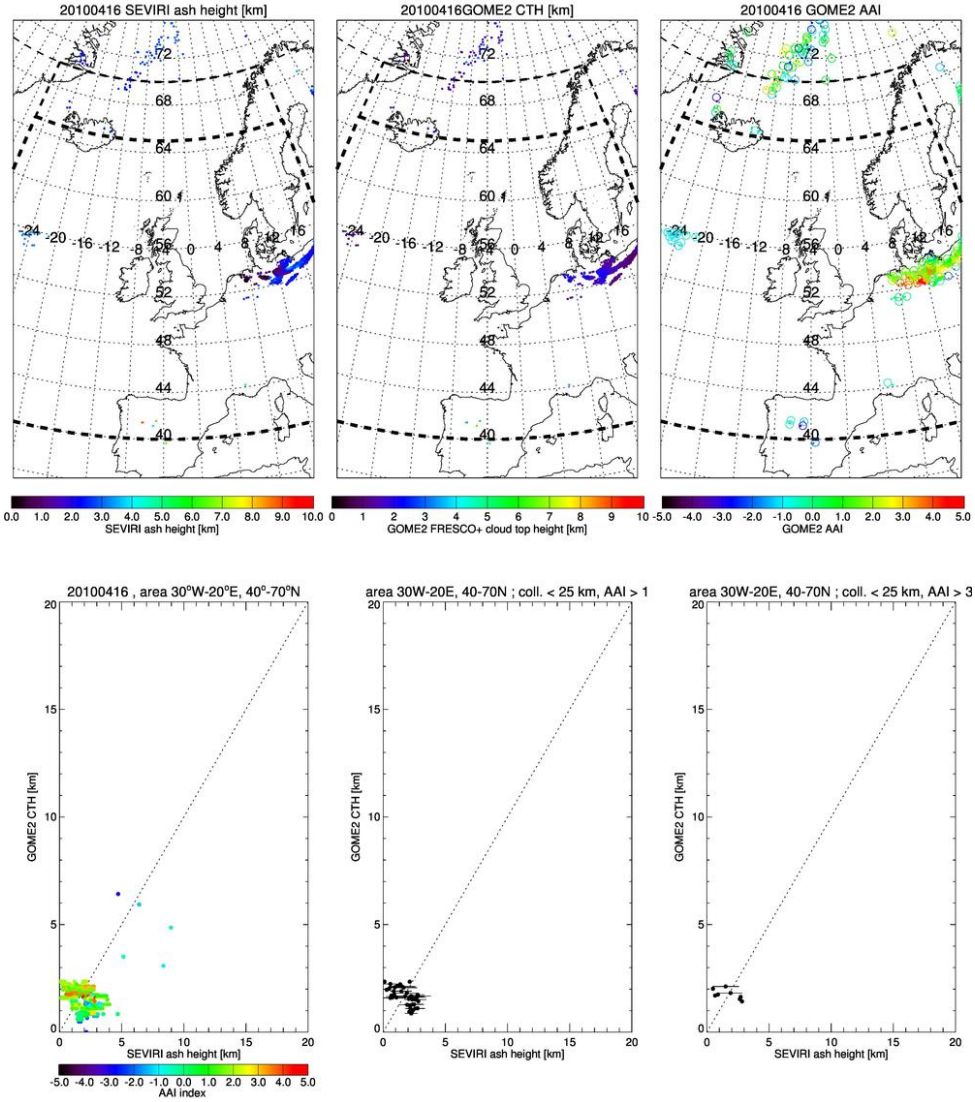

Figure S3-02. 16 April 2010.

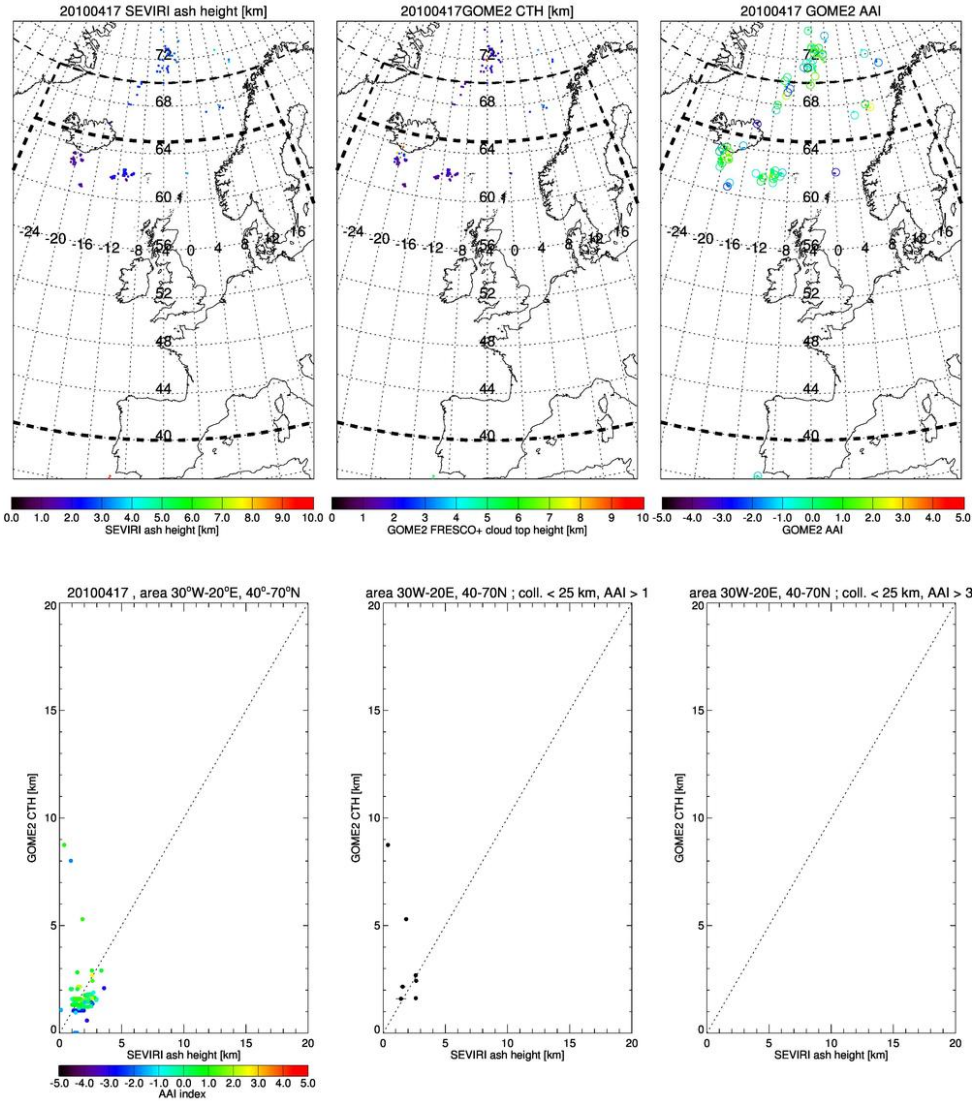

Figure S3-03. 17 April 2010.

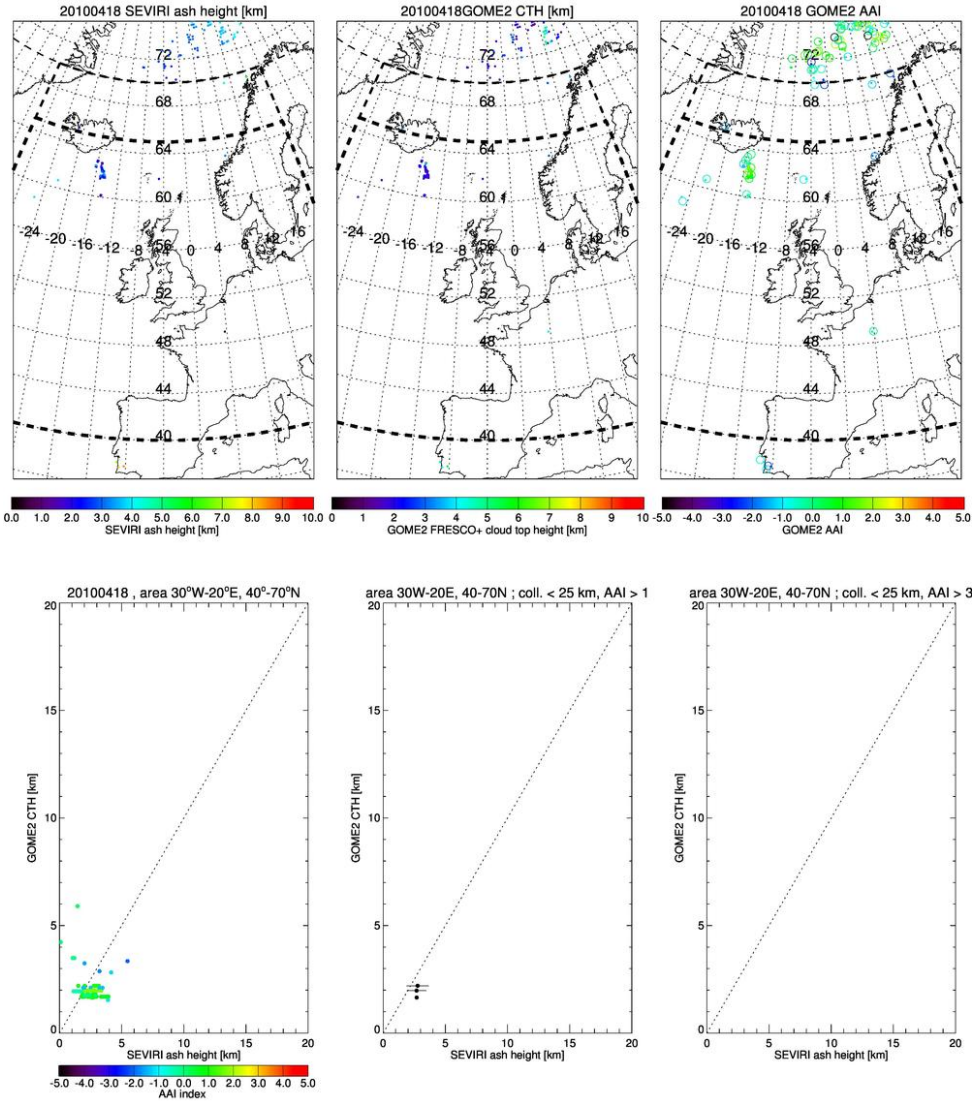

Figure S3-04. 18 April 2010.

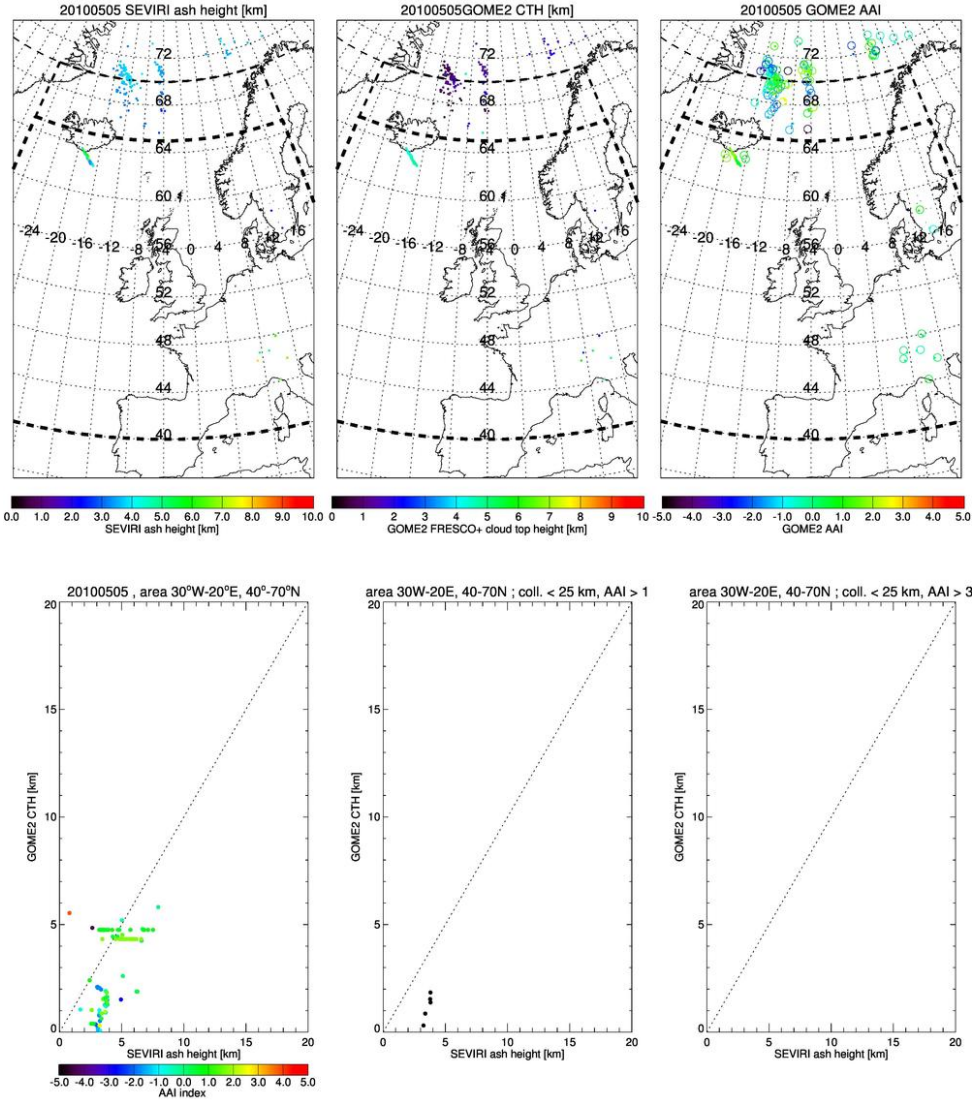

Figure S3-05. 5 May 2010.

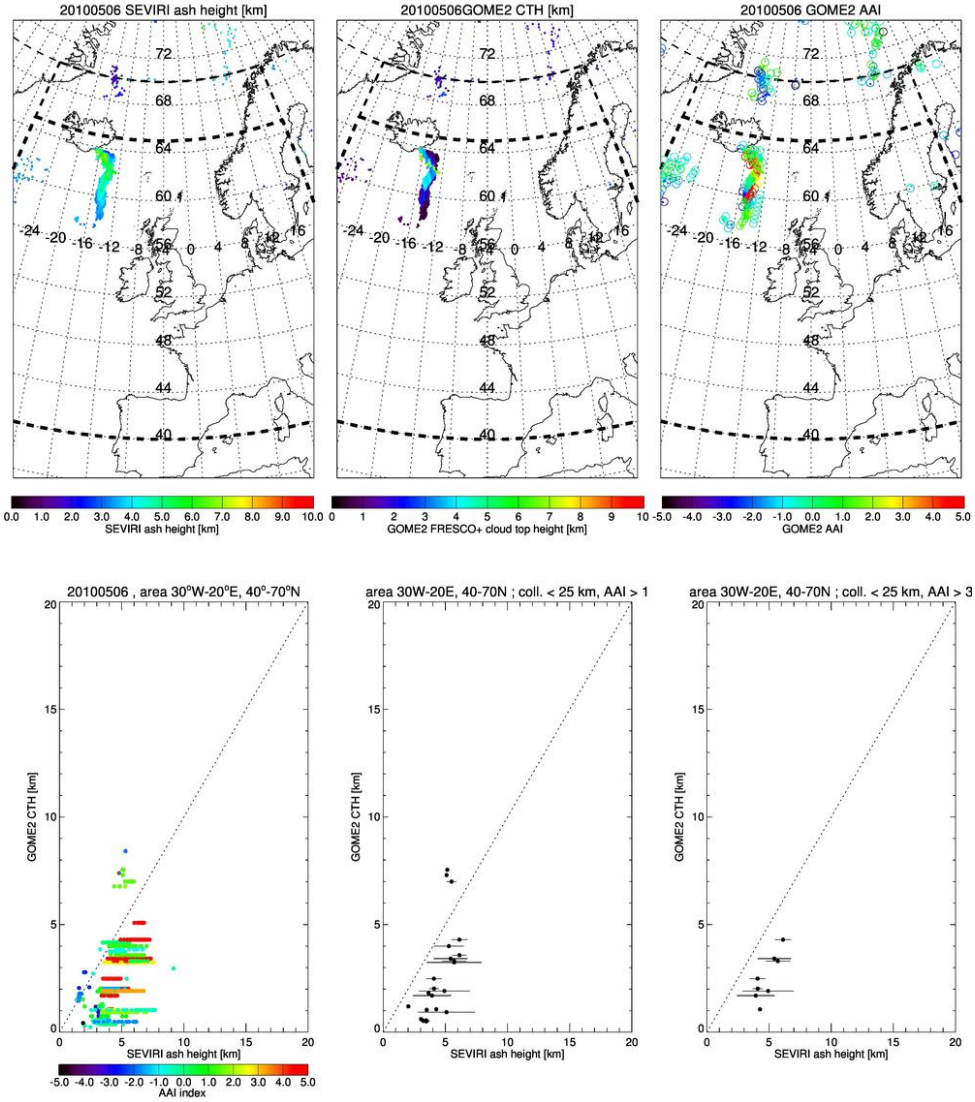

Figure S3-06. 6 May 2010.

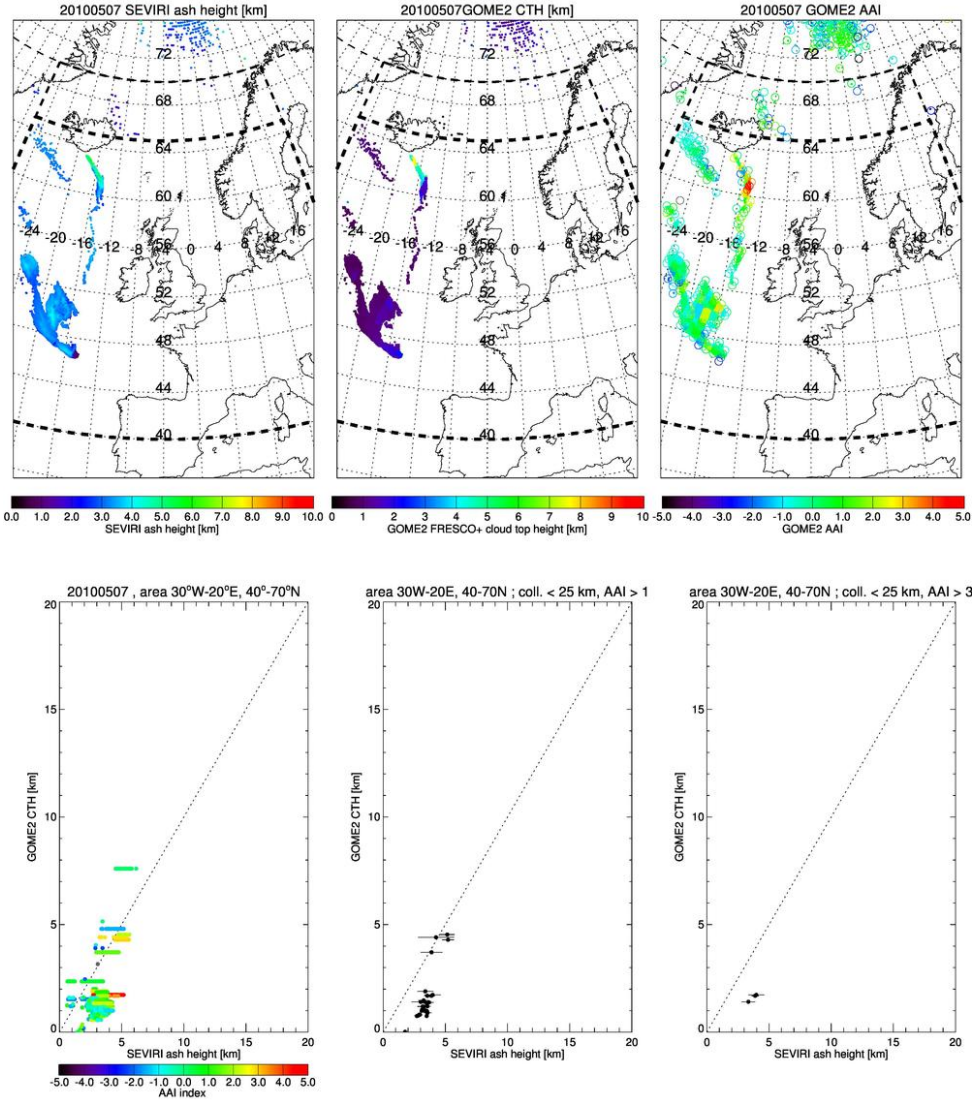

Figure S3-07. 7 May 2010.

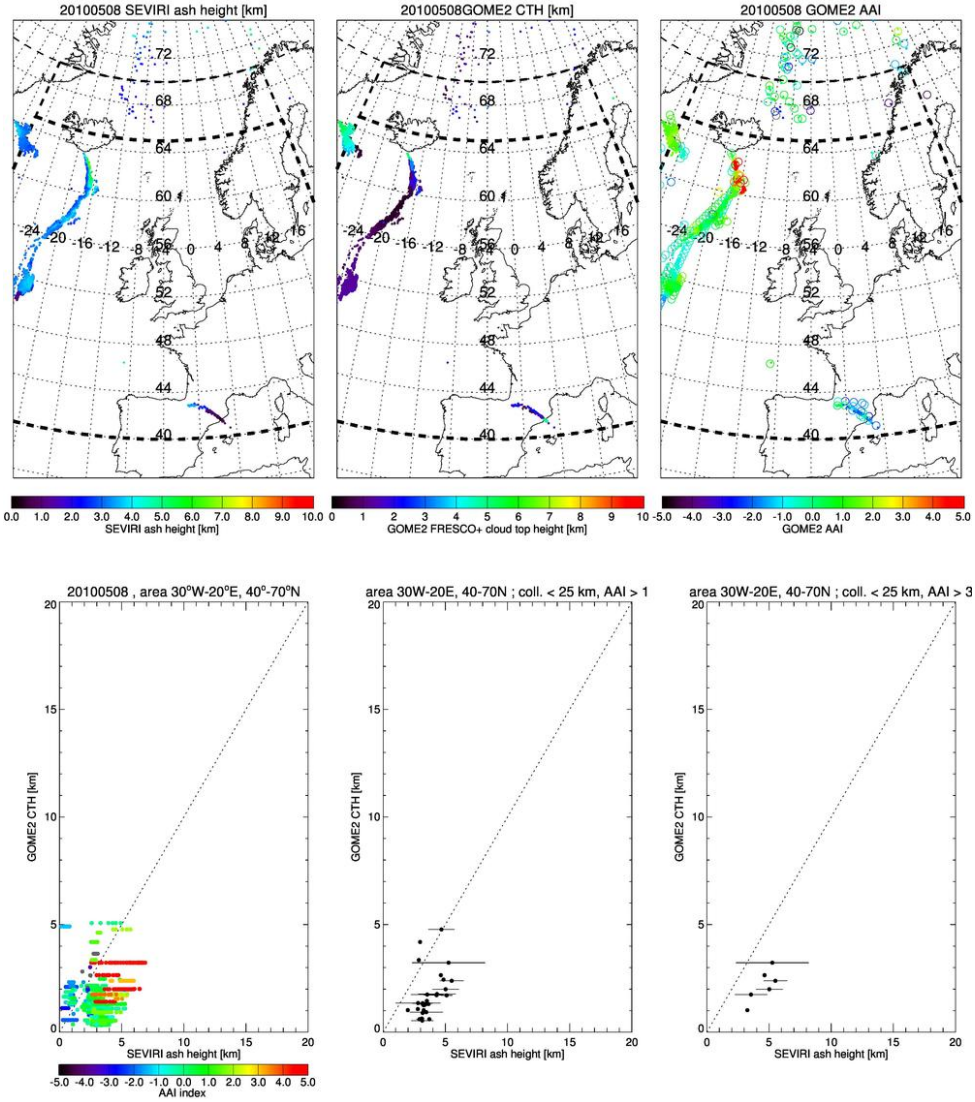

Figure S3-08. 8 May 2010.

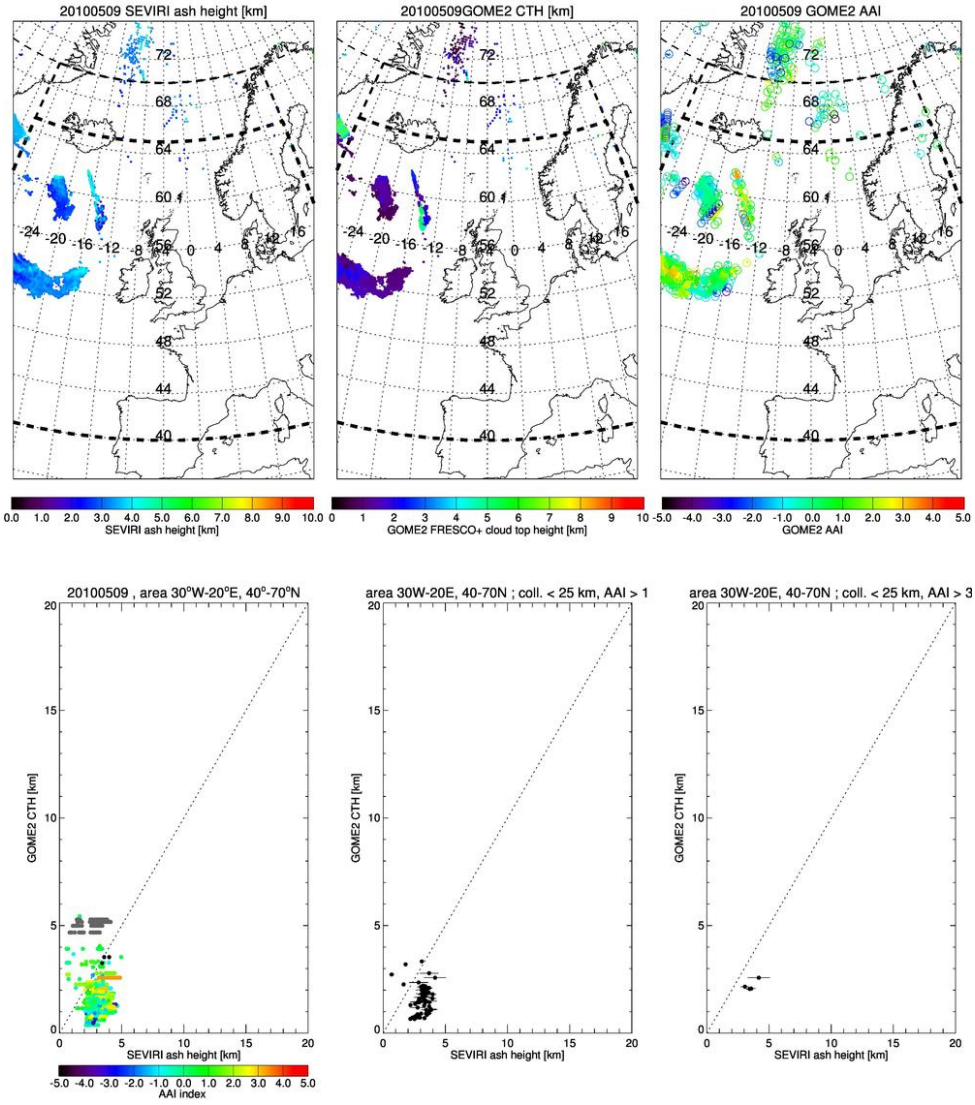

Figure S3-09. 9 May 2010.

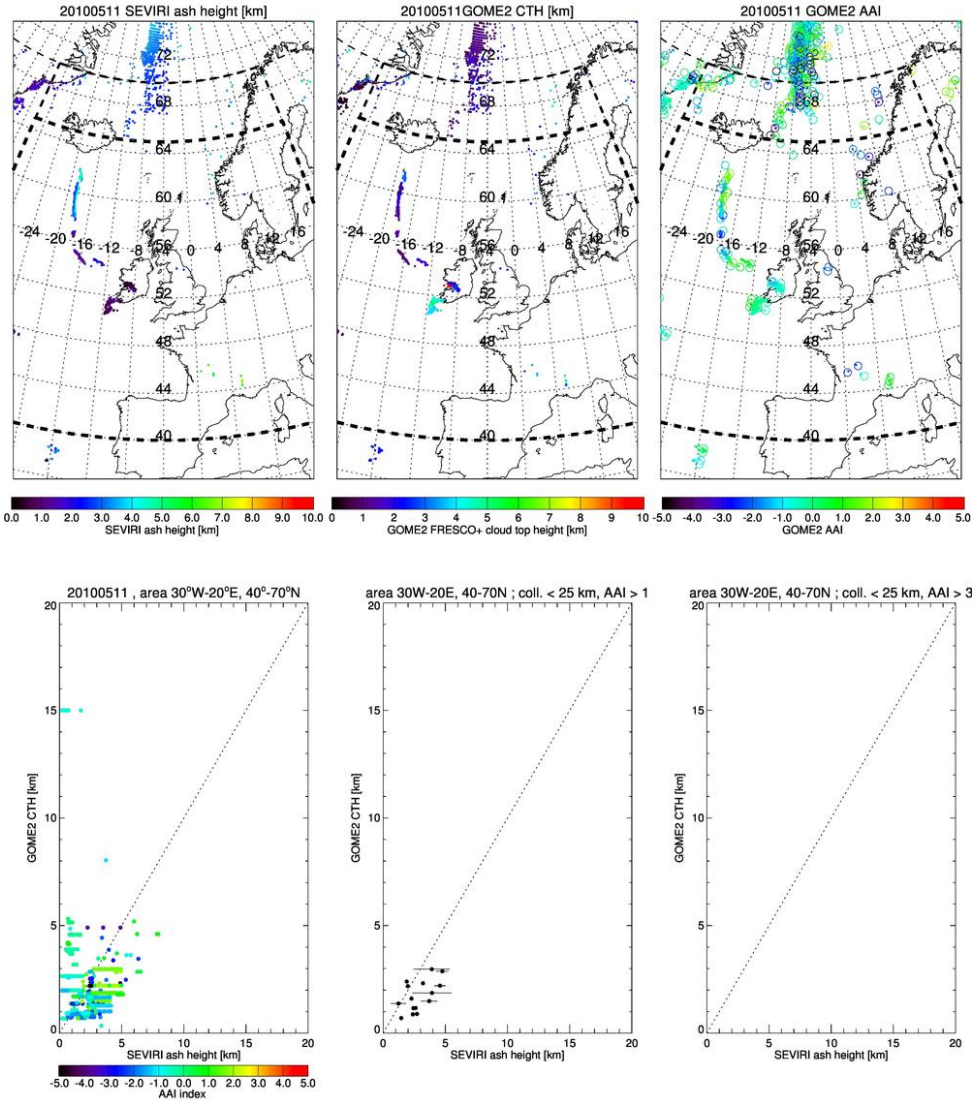

Figure S3-10. 11 May 2010.

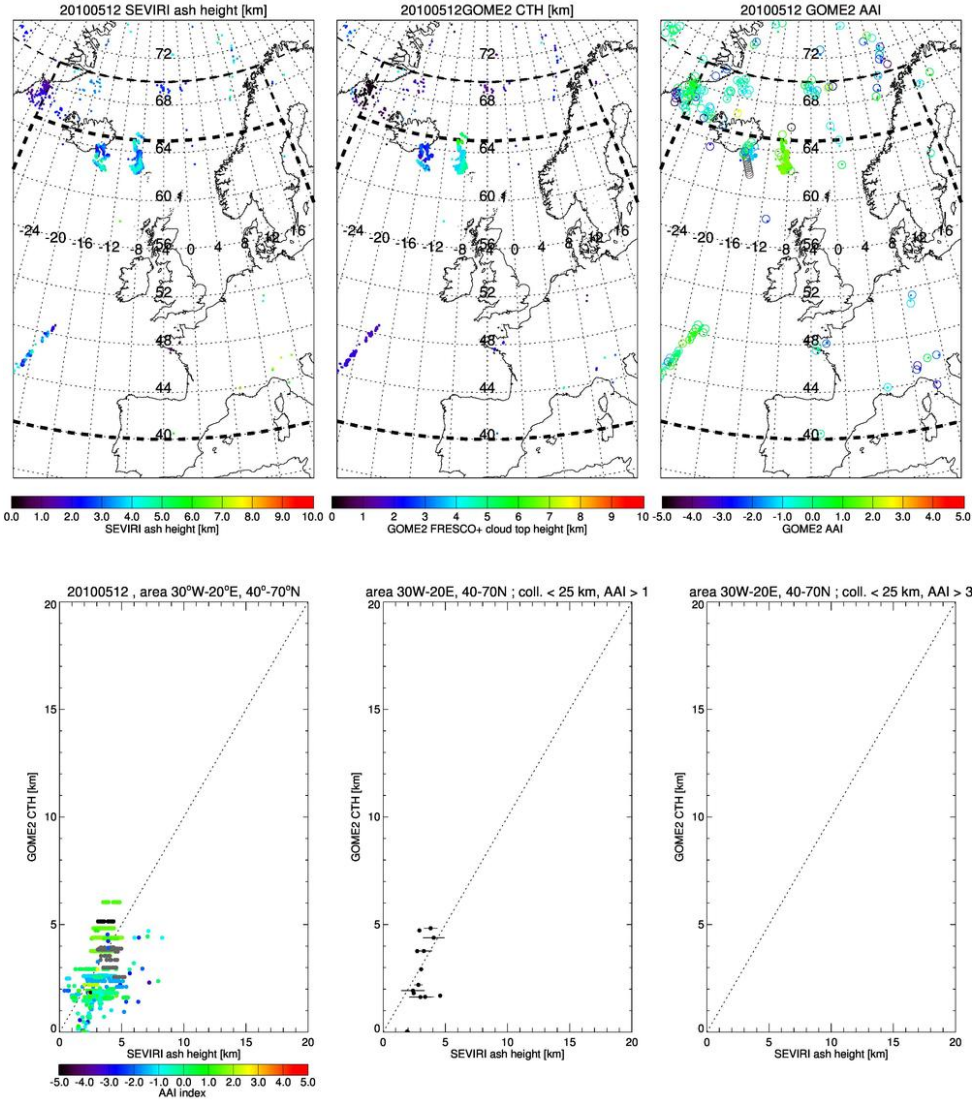

Figure S3-11. 12 May 2010.

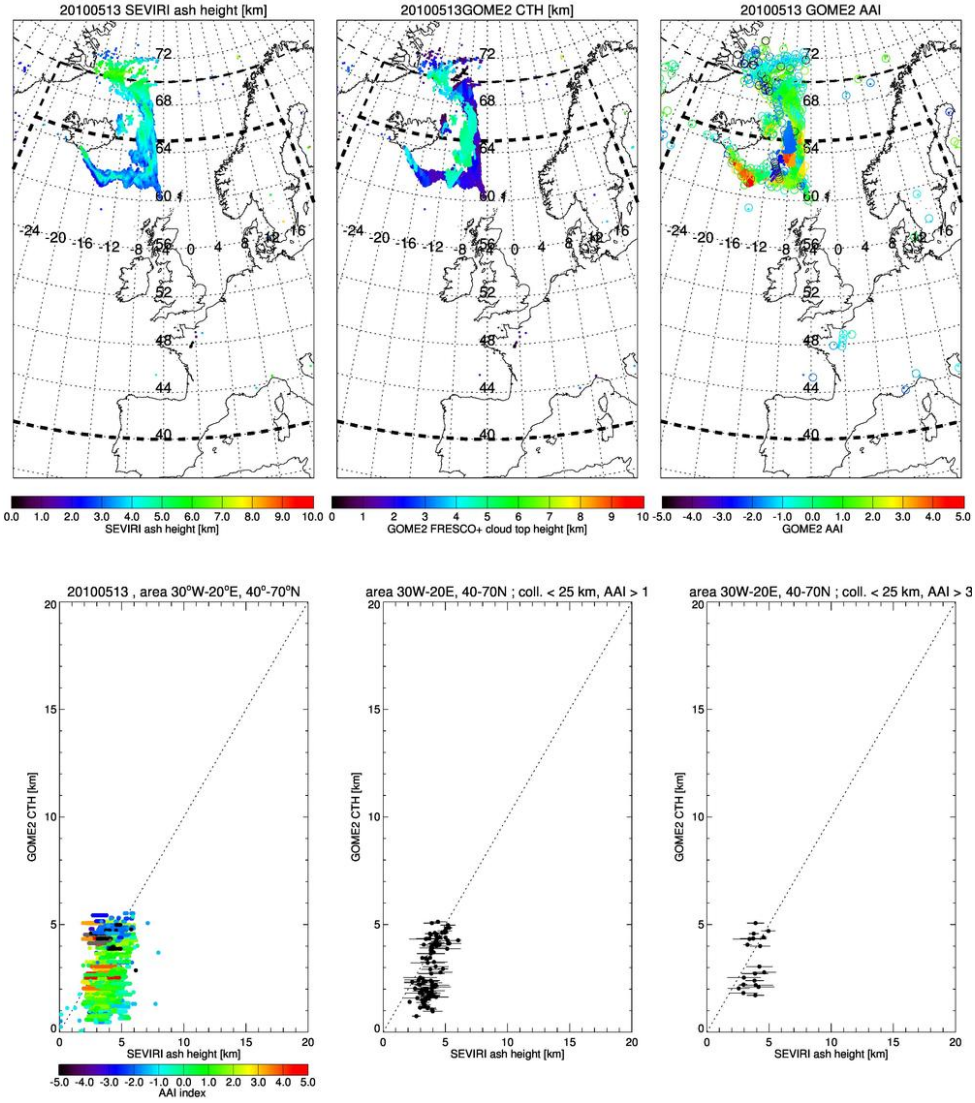

Figure S3-12. 13 May 2010.

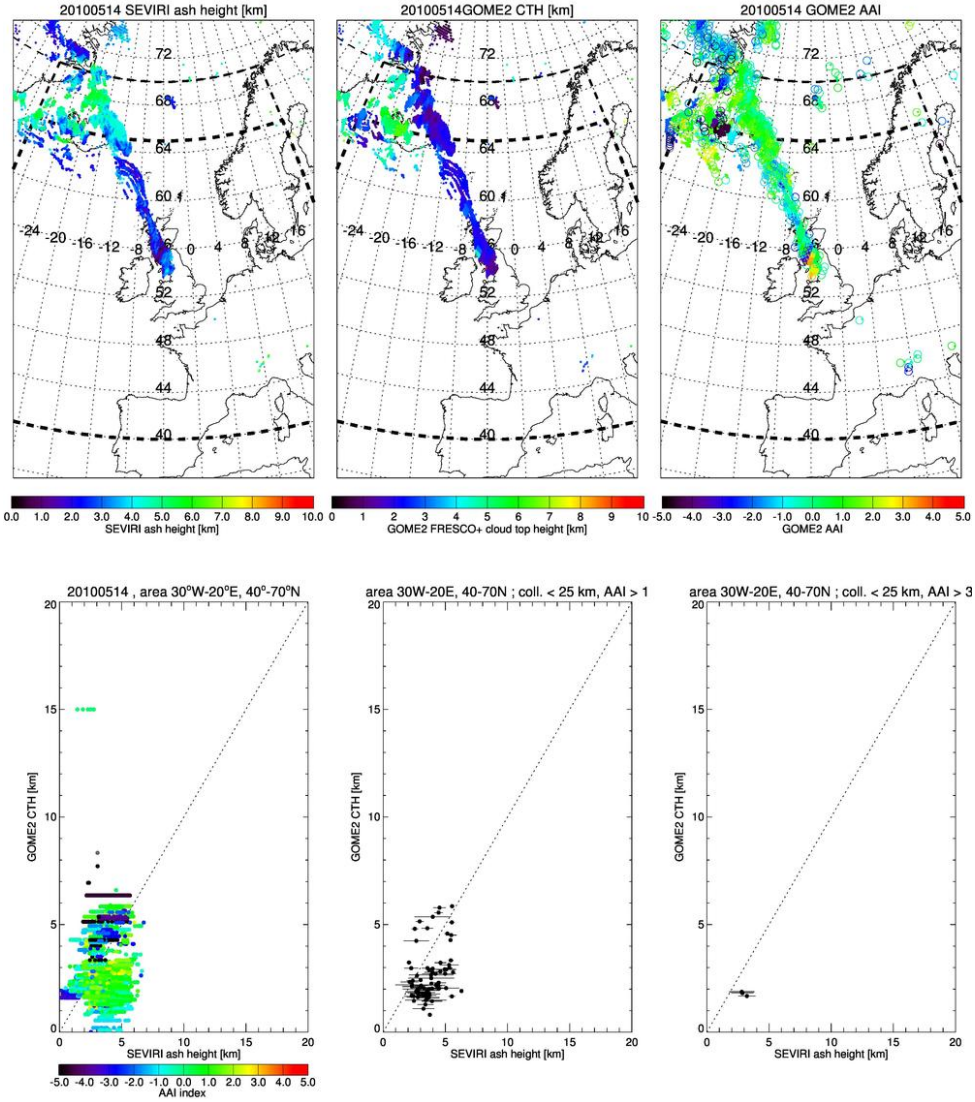

Figure S3-13. 14 May 2010.

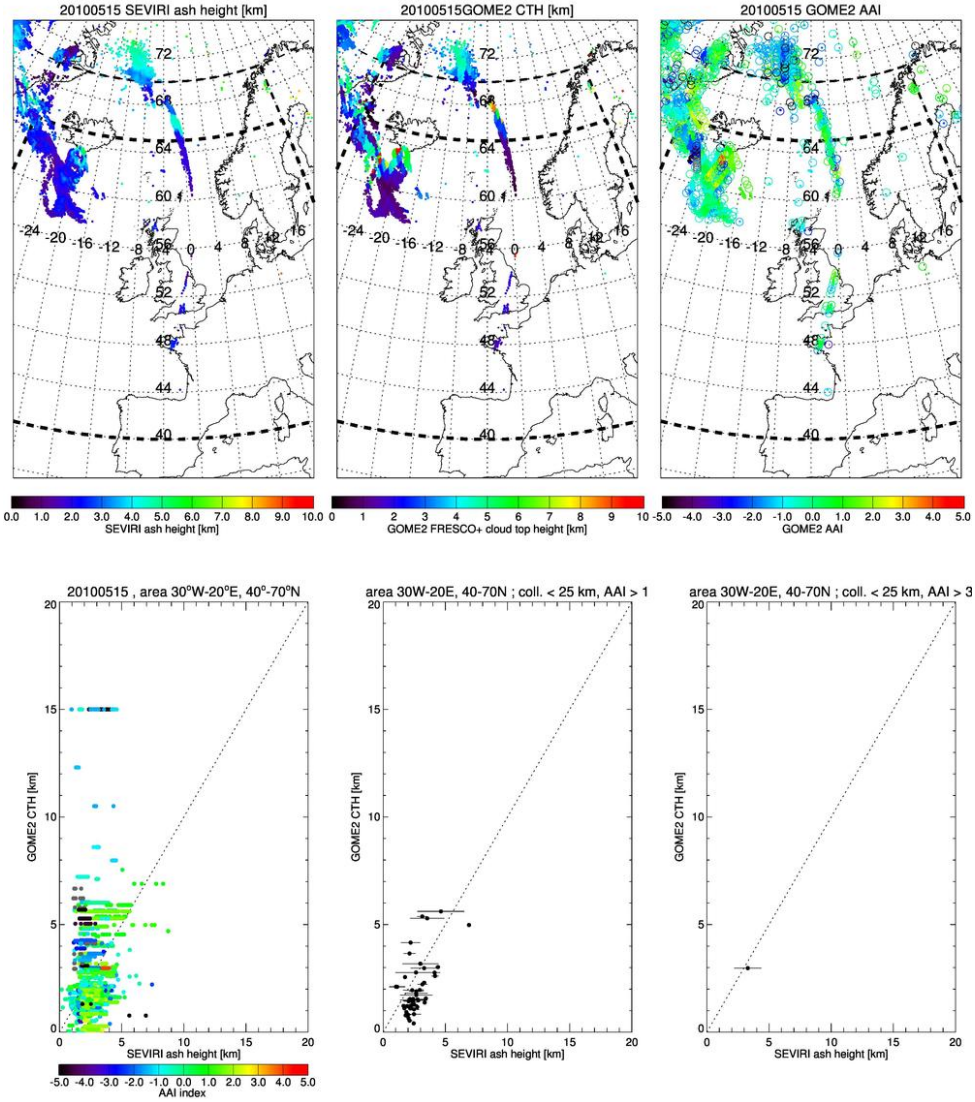

Figure S3-14. 15 May 2010.

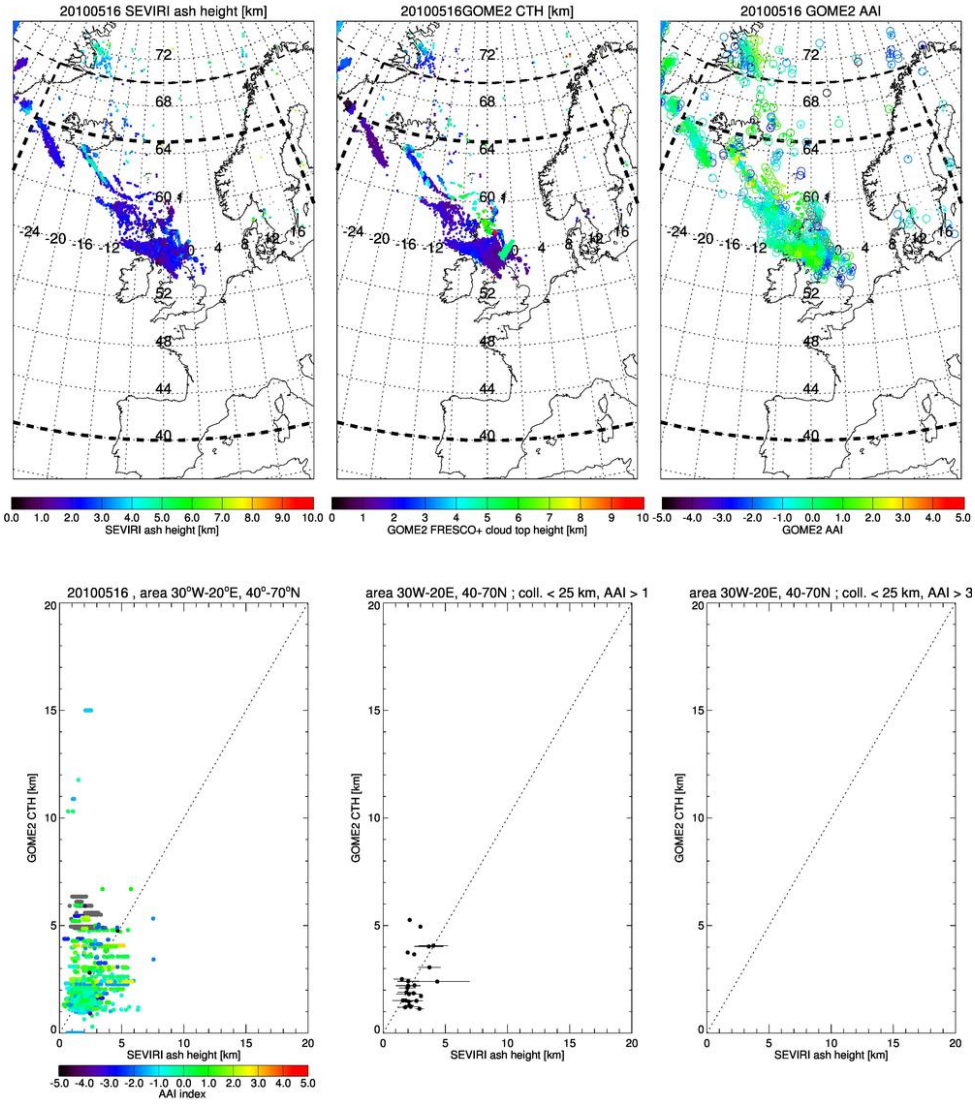

Figure S3-15. 16 May 2010.

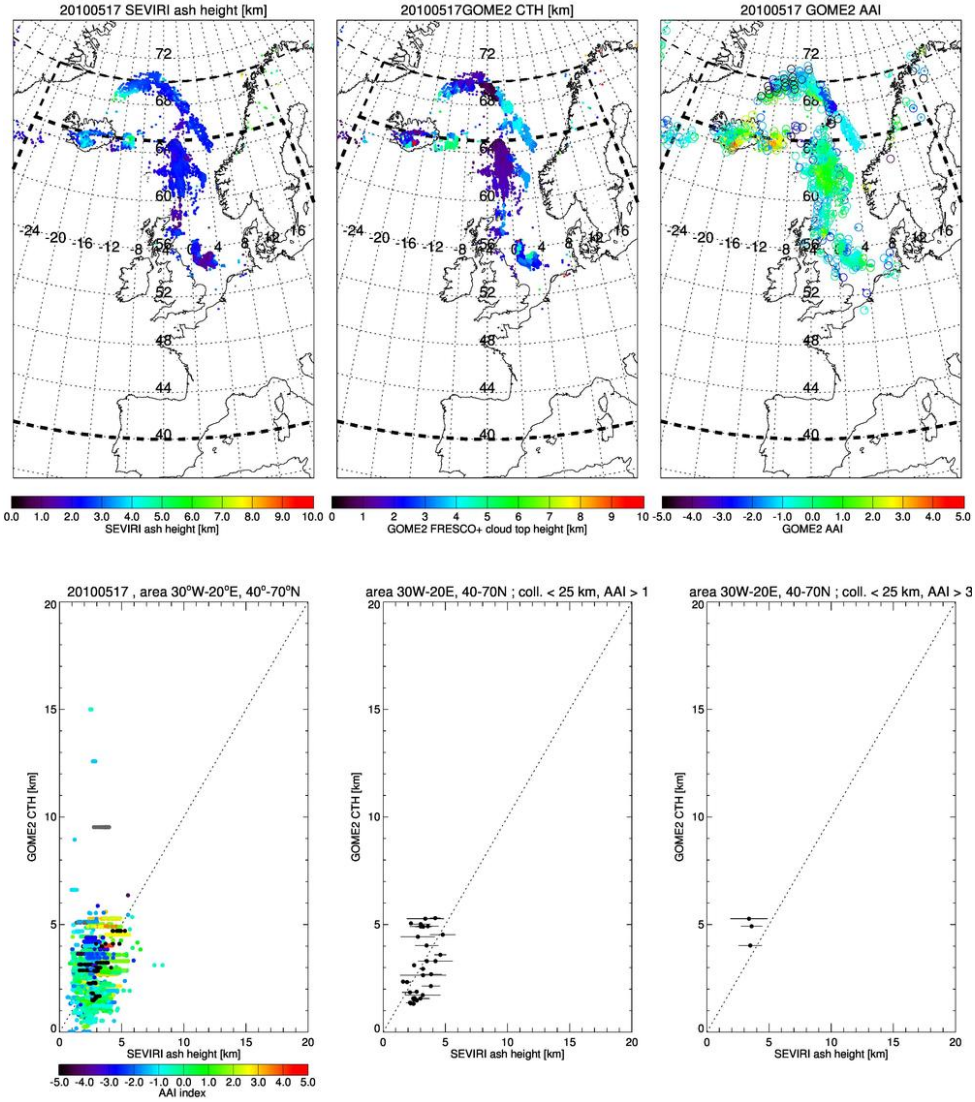

Figure S3-16. 17 May 2010.

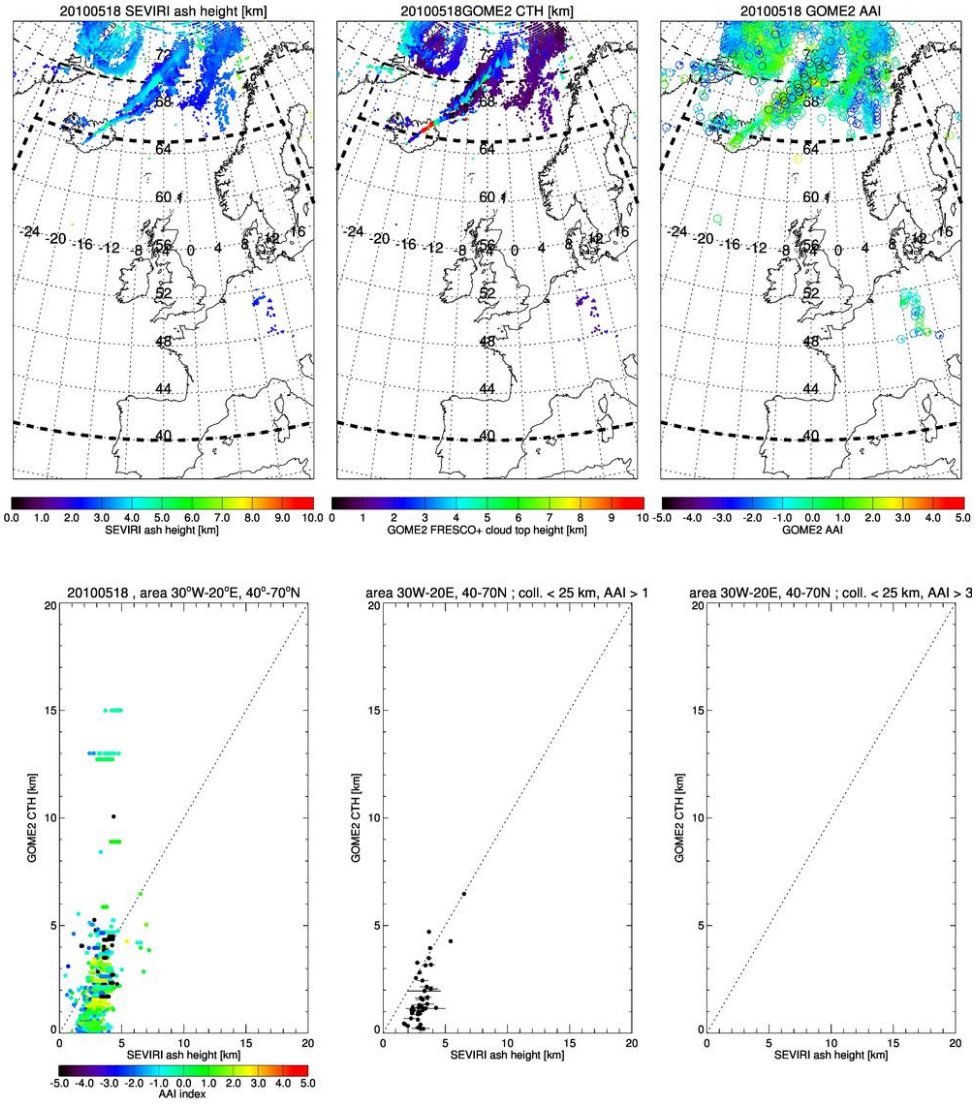

Figure S3-17. 18 May 2010.

A complete list of all KNMI-publications (1854 – present) can be found on our website

www.knmi.nl/knmi-library/knmipub_en.html

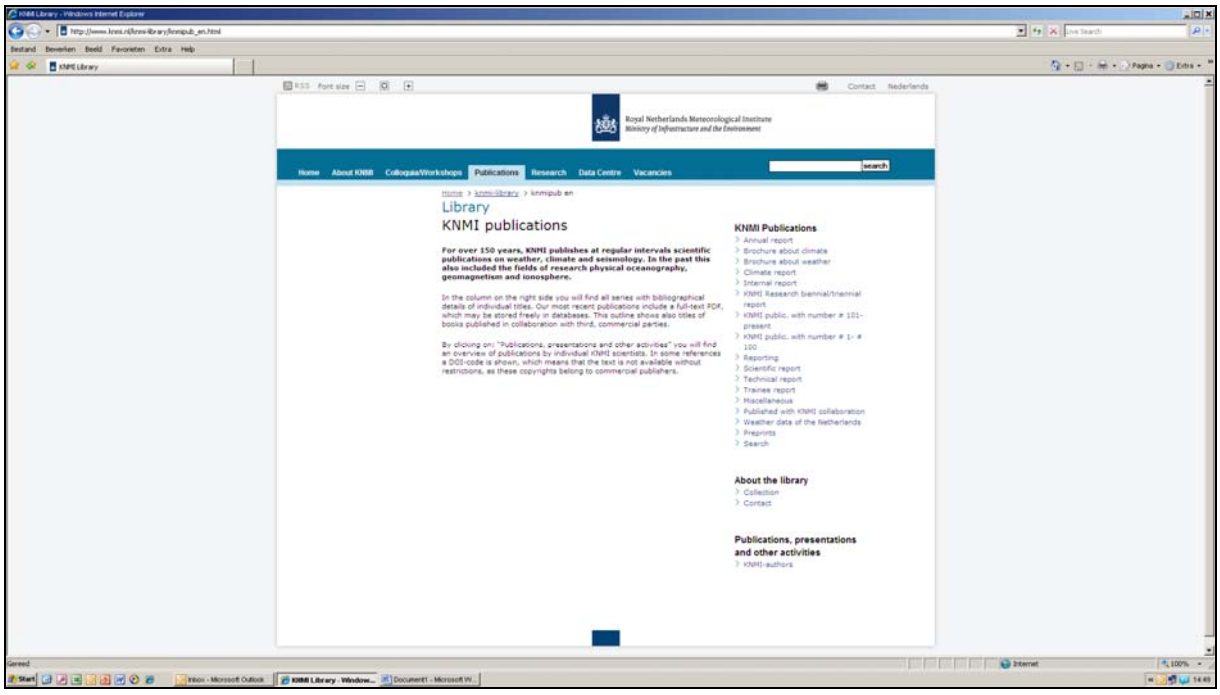

The most recent reports are available as a PDF on this site.